

FY 2011

**Z-SOURCE/CURRENT SOURCE INVERTER–TOPOLOGY
ANALYSIS, COMPARISON AND DESIGN**

Prepared by:

Oak Ridge National Laboratory

Mitch Olszewski, Program Manager

Submitted to:

Energy Efficiency and Renewable Energy
FreedomCAR and Vehicle Technologies
Vehicle Systems Team

Susan A. Rogers, Technology Development Manager

Energy and Transportation Science Division

**Z-SOURCE/CURRENT SOURCE
INVERTER-TOPOLOGY ANALYSIS,
COMPARISON AND DESIGN**

Dong Cao
Fang Z. Peng

Michigan State University

Publication Date: June 2011

Prepared by the
MICHIGAN STATE UNIVERSITY
East Lansing, Michigan 48824-1046
for
UT-BATTELLE, LLC
and the
U.S. DEPARTMENT OF ENERGY
Under contract DE-AC05-00OR22725

DOCUMENT AVAILABILITY

Reports produced after January 1, 1996, are generally available free via the U.S. Department of Energy (DOE) Information Bridge:

Web site: <http://www.osti.gov/bridge>

Reports produced before January 1, 1996, may be purchased by members of the public from the following source:

National Technical Information Service
5285 Port Royal Road
Springfield, VA 22161
Telephone: 703-605-6000 (1-800-553-6847)
TDD: 703-487-4639
Fax: 703-605-6900
E-mail: info@ntis.fedworld.gov
Web site: <http://www.ntis.gov/support/ordernowabout.htm>

Reports are available to DOE employees, DOE contractors, Energy Technology Data Exchange (ETDE) representatives, and International Nuclear Information System (INIS) representatives from the following source:

Office of Scientific and Technical Information
P.O. Box 62
Oak Ridge, TN 37831
Telephone: 865-576-8401
Fax: 865-576-5728
E-mail: reports@osti.gov
Web site: <http://www.osti.gov/contact.html>

This report was prepared as an account of work sponsored by an agency of the United States Government. Neither the United States government nor any agency thereof, nor any of their employees, makes any warranty, express or implied, or assumes any legal liability or responsibility for the accuracy, completeness, or usefulness of any information, apparatus, product, or process disclosed, or represents that its use would not infringe privately owned rights. Reference herein to any specific commercial product, process, or service by trade name, trademark, manufacturer, or otherwise, does not necessarily constitute or imply its endorsement, recommendation, or favoring by the United States Government or any agency thereof. The views and opinions of authors expressed herein do not necessarily state or reflect those of the United States Government or any agency thereof.

Table of Contents

I. Introduction	2
1. Objective and Targets:	2
2. Problem:	2
3. Approach:	3
II. PWM Control method	5
1. Carrier based PWM Control Method	5
2. Space Vector PWM (SVPWM) Control Method	6
III. Topology Analysis and Comparison	7
1. DC analysis and Operation region	7
a. Current-fed Z-source and quasi-Z-source Inverters	7
b. Current-fed Trans-Z-source and Trans-quasi-Z-source Inverters	16
2. Total Device Stress Ratio	22
a. TSDPSR of the four topologies using P_o as the power base in terms of D_{op} :	22
b. TSDPSR of the four topologies using $V_{\max} I_{l_rms}$ as the power base in terms of M:	23
c. TSDPSR of the four Topologies Using $V_{\max} I_{l_rms}$ as the power base in terms of D_{op}	24
3. Passive Components Design	25
a. Current-fed Quasi-Z-source Inverter (CF-qZSI)	25
b. Current-fed Z-source Inverter (CF-ZSI)	32
c. Current-fed Trans-quasi-Z-source Inverter (CF-trans-qZSI)	38
d. Current-fed Trans-Z-source Inverter (CF-trans-ZSI)	46
IV. 55 kW Current-fed Inverter Design	54
1. Design Specifications:	54
2. Design Procedures:	54
a. Switching Device:	55
b. Diode:	60
c. Z-source Capacitor	63
d. Z-source Inductor	68
e. Input Inductor	76
f. Output Filter Capacitor	82
g. Heatsink	83
3. Conclusion	83

I. INTRODUCTION

1. Objective and Targets

The objective of this research is to further reduce the cost, volume and weight of the present power electronics (PE) system in the hybrid electric vehicle (HEV) by 25%. The Toyota Camry PE system is used as the reference. The research efforts will address achieving the 2015 power electronics targets: \$5/kW, 12 kW/kg, 12 kW/L.

Four current-fed Z-source inverter topologies will be analyzed and compared. Distinct features of the current-fed Z-source inverters will be proposed and summarized. The PWM control methods will be proposed and compared. One of the current-fed Z-source inverters will be selected for the simulation study and the 55 kW prototype design. The feasibility of the current-fed Z-source inverter for the HEV motor drive, including boost, inverter, regeneration, and Plug in HEV charging functions will be verified by simulation. A performance metrics in terms of power density (kW/L), specific power (kW/kg) and efficiency characteristics of this prototype will be estimated and generated. The design barriers and key points will be summarized for the future optimized design tasks.

2. Problem

The traditional voltage source inverter (VSI) has many drawbacks. Fig. 1 shows the traditional three phase VSI motor drive system. Fig. 2 shows the one phase output voltage of the traditional VSI. Because the output voltage waveform of the traditional VSI is pulse voltage with sinusoid pulse width modulation. The pulse voltage output voltage of the VSI will cause the high EMI noises, high stress on the motor insulation, high frequency core and copper losses of the motor and bearing leakage currents.

Also, a bulky dc bus capacitor has to be adopted in the VSI, because of the high the current stress in the dc capacitor. In order to satisfy the current stress requirement, many capacitors have to be put in parallel to reduce the capacitor total ESR and prevent significant temperature rise.

In traditional VSI, the two switches connected in one phase leg have to be controlled complementary to prevent the short circuit of the dc bus capacitor. The possible shoot through will cause long term reliability concerns. Also, a deadtime has to be added to the control of the two switches in one phase leg to avoid the shoot-through. The inserted deadtime will cause the distortion of the output voltage.

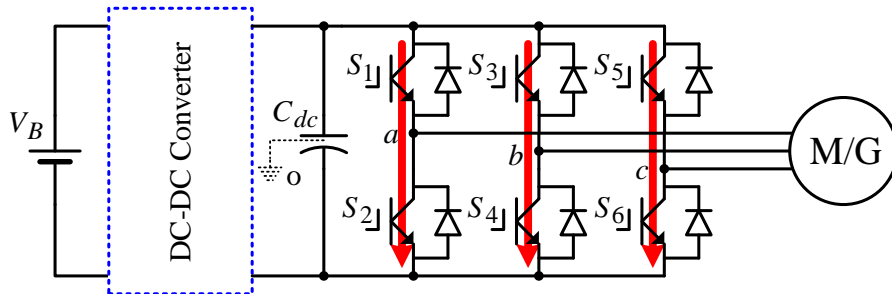


Fig. 1. Traditional VSI for motor drive circuit with potential device shoot-through failures.

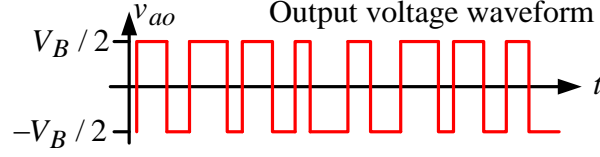


Fig. 2. One phase output voltage of traditional VSI.

For the VSI, the peak output line-to-line voltage is the dc-link capacitor voltage. If the battery is connected directly in parallel with the dc-link capacitor, the peak output voltage of the VSI is limited by the battery voltage. Also, the battery output voltage will change due to the battery state of charge. In order to output high output voltage, a high voltage battery with enough margin has to be adopted, which will increase the cost and reduce the reliability. So a separate dc-dc boost converter is usually needed for the voltage boosting and regulation, as shown in Fig. 1. This boost dc-dc converter will add extra cost and reduce the system reliability.

3. Approach

In order to overcome the abovementioned problems of voltage source inverter. This research concentrates on the current-fed inverters (CSI) with a passive Z-source network, as shown in Fig. 3. Only inductor, capacitor and diode are used in the Z-source network. There are several unique features of current-fed Z-source inverter.

Compared to the traditional CSI, the current fed inverter can achieve buck and boost function in single stage. Because traditional CSI can only boost the input voltage, an extra interfacing circuit with active switches has to be implemented to output lower voltage and achieve the buck function. Also, the traditional CSI cannot perform the open circuit event, at least one loop with two devices conducting has to be assured. But the current-fed Z-source inverter can have the open circuit during the operation which means every phase leg is tolerant to shoot-through and open circuit. The current-fed Z-source inverter can also achieve battery charging function during the motor regeneration mode.

Compared to the traditional VSI, because of the using of reverse-blocking (RB) IGBT, the anti-parallel diodes existing in the VSI could be eliminated. The total capacitance could be reduced, because no bulky capacitor bank is need anymore. Similar to the traditional CSI, the output voltage and current of the current-fed Z-source inverter are sinusoid, as shown in Fig. 4 thus reduce the voltage stress of the motor. The constant-power speed range can be extended without using extra boost converter thus reducing the system cost.

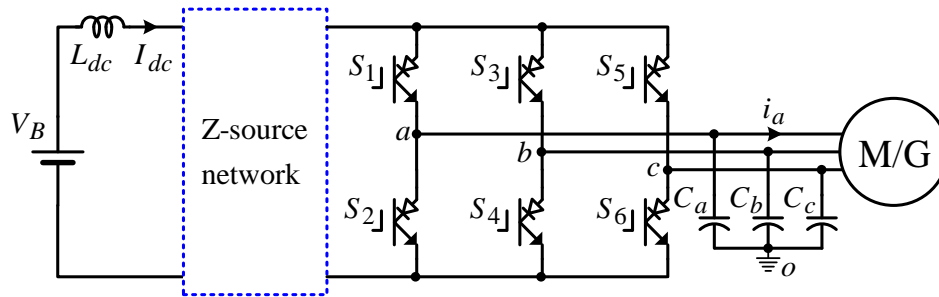


Fig. 3. Main circuit of the current-fed inverter with a passive Z-source network.

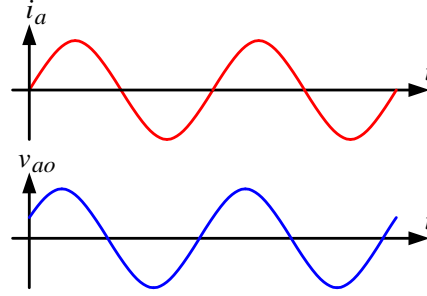


Fig. 4. Output phase voltage and line current of the current-fed inverter with a Z-source network.

There are four different current-fed Z-source inverters, as shown in Fig. 5, Fig. 6, Fig. 7, and Fig. 8. Fig. 5 and Fig. 6 show the two current-fed Z-source inverters with different Z-network, but their Z-network are both composed of two inductors, two capacitors and a diode. According to the difference of the Z-network, they are called current-fed quasi-Z-source inverter and current-fed Z-source inverter respectively. Fig. 7 and Fig. 8 show other two current-fed Z-source inverters with coupled inductor/transformer. Compared to the previous two, these two inverters only have one capacitor, and the transformer turns ratio can be increased to even extend the constant power range with higher boost ratio. In the following sections, these four topologies are analyzed and compared in terms of control, operation range, switching device stress, passive components stress, etc. one of the topology will be chosen for the simulation study and 55 kW prototype design.

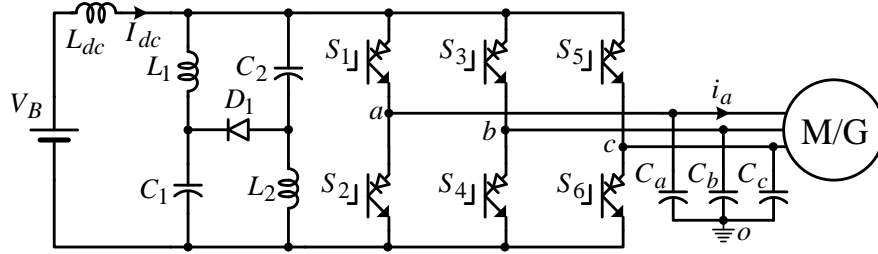


Fig. 5. Current-fed quasi-Z-source inverter main circuit.

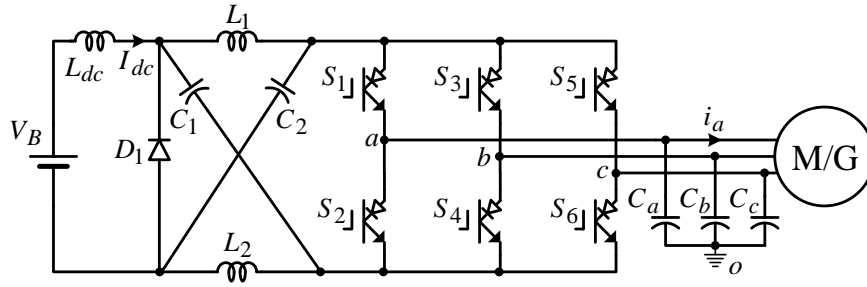


Fig. 6. Current-fed Z-source inverter main circuit.

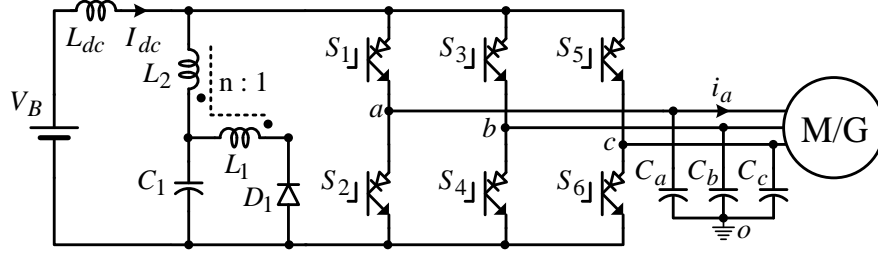


Fig. 7. Current-fed trans-quasi-Z-source inverter main circuit.

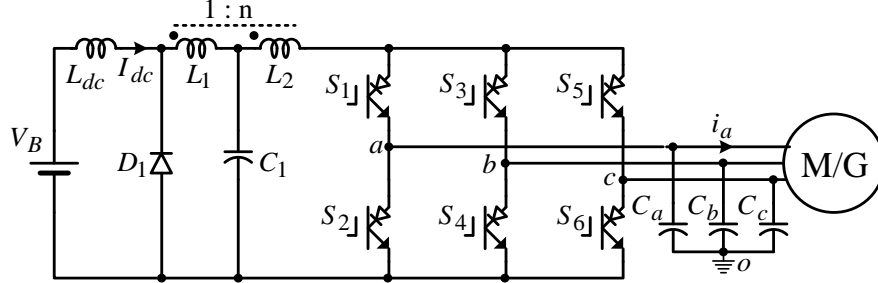


Fig. 8 Current-fed trans-Z-source inverter main circuit.

II. PWM CONTROL METHOD

1. Carrier based PWM Control Method

Compared to the traditional CSI control method [1], two open circuit zero state references are added in the reference, as shown in Fig. 9. During this period, the shoot-through zero state, as shown in Fig. 9 when S_1 and S_2 are both conducting are changed to open state zero state. Similar to the voltage fed Z-source inverter, there are several methods we can insert the open circuit zero state based on the different open zero state reference choices. We can call it simple boost control by only add two straight lines as the open circuit zero state reference, maximum boost control by using the envelop of the three phase current reference, and constant boost control by using a 3ω sinusoid reference, as shown in Fig. 10. The maximum boost control transfer all the shoot through zero state to open circuit zero state. The simple boost control and the constant boost control have the same open state duty cycle in every switching cycle. Compare to the simple boost control, the constant boost control transfers most shoot-through zero state into open circuit zero state while keeping the open circuit zero state constant in every switching cycle. The constant boost control has the same result as the simple boost control with third harmonic rejection.

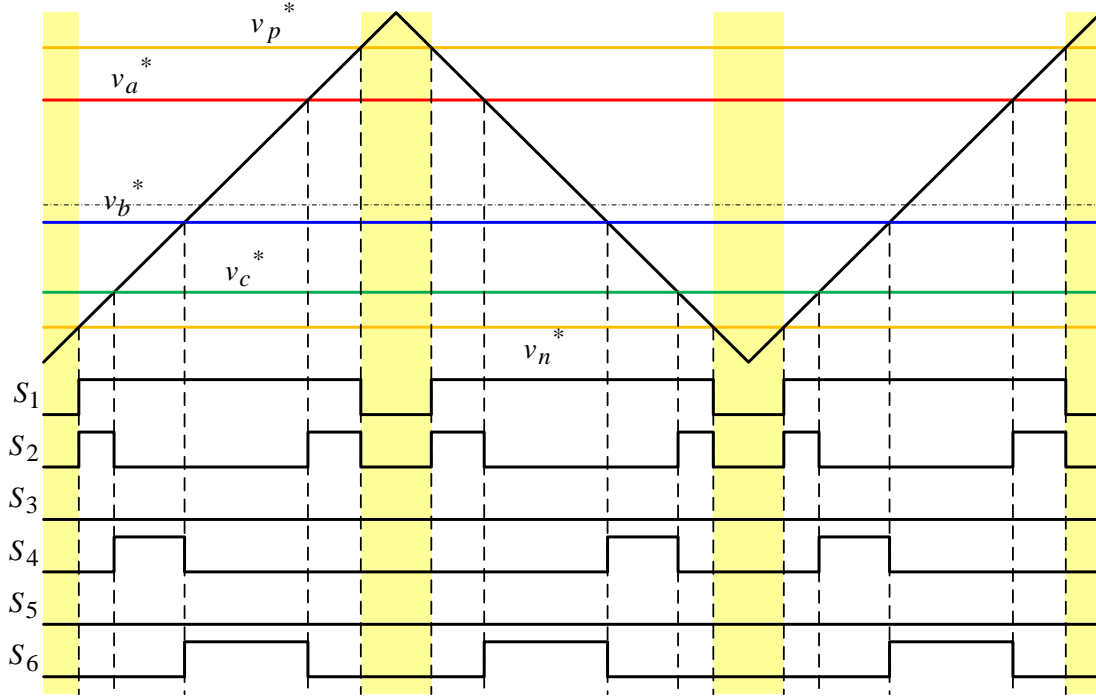


Fig. 9. PWM control method with open circuit zero state inserted.

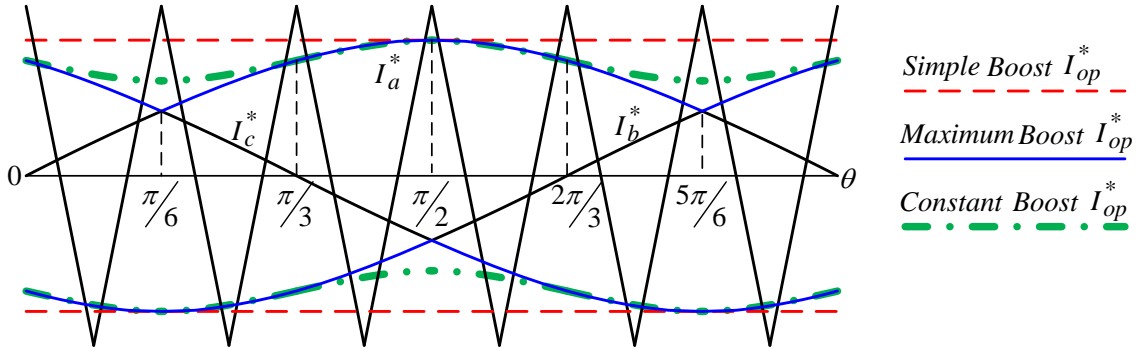


Fig. 10. Three different PWM control method using different open zero state reference.

2. Space Vector PWM (SVPWM) Control Method

The SVPWM for Z-source inverter has been discussed in detail in [2], which will not be discussed here. Similarly to the carrier based methods, the point of the SVPWM control for Current-fed Z-source inverters is transferring the original shoot-through zero state into open circuit zero state to achieve the buck function.

III. TOPOLOGY ANALYSIS AND COMPARISON

1. DC Analysis and Operation region

a. Current-fed Z-source and quasi-Z-source Inverters

1. DC analysis using three switching states with corresponding duty cycle

Fig. 11 shows the equivalent circuits of current-fed quasi-Z-source inverter (CF-qZSI) viewed from the dc link. There are three dc operation states, as shown in Fig. 11 (a), (b), and (c). Fig. 11(a) shows the state I, the active state. During this state, the inverter is in one of the six active states, which is equivalent to a dc voltage source. The diode D_1 is not conducting. Fig. 11(b) shows the state II, the shoot through zero state. During this state, one of the inverter bridge is shorted. The diode D_1 is not conducting. Fig. 11(c) shows the state III, the open circuit zero state. During this state, all the switches of the inverter is off, and the inverter is equivalent to an open circuit. The diode D_1 is conducting during this state. And Fig. 12 shows the similar three dc equivalent circuits of current-fed Z-source inverter (CF-ZSI)

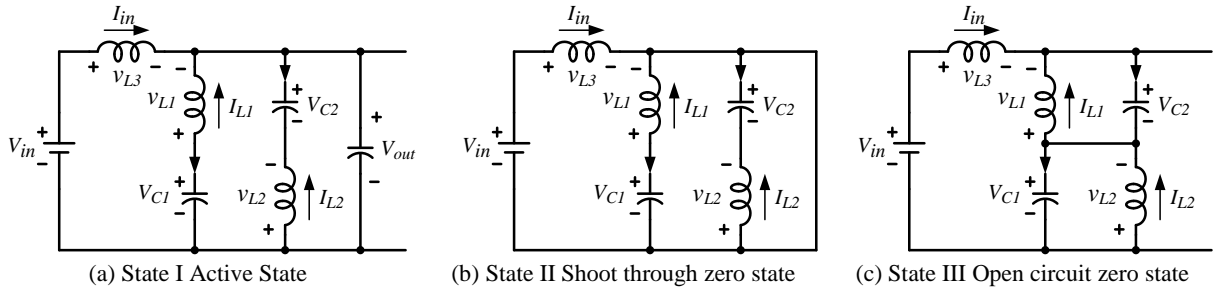


Fig. 11. Equivalent circuit of CF-qZSI.

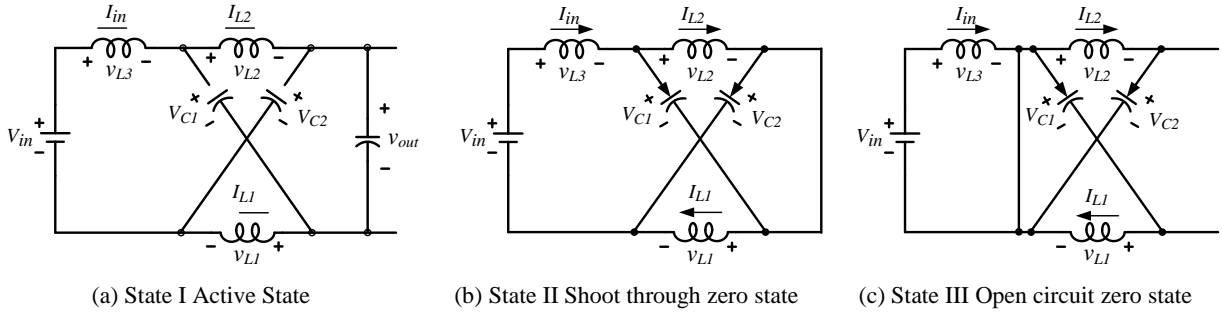


Fig. 12 Equivalent circuit of CF-ZSI.

According to Fig. 11, we can derive the dc steady state equations as follows. Assume the capacitor C_1 and C_2 and the inductor L_1 and L_2 in the Z-source network have the same capacitance and the same inductance respectively. According to the circuit symmetry, Kirchhoff's law of the equivalent circuit, the capacitor charge balance and the inductor voltage second balance. We can have the following dc equations, as shown in (1). The D_A is the duty cycle of the active state. D_{sh} is the duty cycle of the shoot-through state, and D_{op} is the duty cycle of the open circuit zero state:

$$\begin{cases} V_{C1} = V_{C2} = V_C; v_{L1} = v_{L2} = v_L \\ V_{C1} + v_{L1} = V_{C2} + v_{L2} = V_{in} + v_{L3} \\ (V_{in} - V_{out})D_A + V_{in}D_{sh} - V_{in}D_{op} = 0 \\ -I_{L1}D_A + (-I_{L1})D_{sh} + (I_{L2} + I_{in})D_{op} = 0 \\ -I_{L2}D_A + (-I_{L2})D_{sh} + (I_{L1} + I_{in})D_{op} = 0 \\ D_A + D_{sh} + D_{op} = 1 \end{cases} \quad (1)$$

By solving the equation group (1), we can have the following results

$$\frac{I_{L1}}{I_{in}} = \frac{I_{L2}}{I_{in}} = \frac{D_{op}}{D_{sh} + D_A - D_{op}} = \frac{D_{op}}{1 - 2D_{op}} \quad (2)$$

$$\frac{V_{out}}{V_{in}} = \frac{D_A + D_{sh} - D_{op}}{D_A} = \frac{1 - 2D_{op}}{D_A} \quad (3)$$

$$\frac{V_{out}}{V_{in}} = \begin{cases} \frac{1}{D_A} & \text{if } D_{op} = 0 \\ \frac{2D_A - 1}{D_A} & \text{if } D_{sh} = 0 \end{cases} \quad (4)$$

According to Fig. 12, based on the same assumption of Fig. 11, we can similarly have the capacitor charge balance and inductor voltage second equation group as follows:

$$\begin{cases} V_{C1} = V_{C2} = V_C; v_{L1} = v_{L2} = v_L \\ V_{C1} + v_{L1} = V_{C2} + v_{L2} = V_{in} + v_{L3} \\ (-V_{in} + V_{out})D_A - V_{in}D_{sh} + V_{in}D_{OP} = 0 \\ (I_{in} - I_{L2})(D_A + D_{sh}) + I_{L1}D_{OP} = 0 \\ (I_{in} - I_{L1})(D_A + D_{sh}) + I_{L2}D_{OP} = 0 \\ D_A + D_{sh} + D_{OP} = 1 \end{cases} \quad (5)$$

By solving the equation group (5), we can have the following results

$$\frac{I_{L1}}{I_{in}} = \frac{I_{L2}}{I_{in}} = \frac{1 - D_{op}}{1 - 2D_{op}} \quad (6)$$

$$\frac{V_{out}}{V_{in}} = \frac{D_A + D_{sh} - D_{op}}{D_A} = \frac{1 - 2D_{op}}{D_A} \quad (7)$$

$$\frac{V_{out}}{V_{in}} = \begin{cases} \frac{1}{D_A} & \text{if } D_{op} = 0 \\ \frac{2D_A - 1}{D_A} & \text{if } D_{sh} = 0 \end{cases} \quad (8)$$

From the above the results, we can derive that, the dc output voltage gain of CF-qZSI and CF-ZSI is the same. Fig. 13 shows the dc voltage gain of CF-qZSI and CF-ZSI. For both of the two topologies, there are three different operation regions. Region B is the motoring region, the inverter equivalent dc output

voltage is between $0 \sim 2V_{in}$. Region C is the regenerative region, because the output voltage gain is negative. In this region, the inverter can operate as a PWM rectifier to charge the input battery. Region A is the prohibited region, if the output voltage gain is larger than two, the diode of the Z-source network will conduct automatically. The output voltage will get distortion due to the unwanted conduction of the diode. If we want to extend the motoring operation region of these two circuits, a reverse blocking switching device will have to be added to replace the diode. Mode 1 is the motoring operation region line without any open circuit zero states, where the highest voltage gain can be achieved. Mode 2 is the regeneration region line where all the shoot through zero states are replaced by the open circuit zero state. During this mode, these two inverters can output the lowest possible voltage.

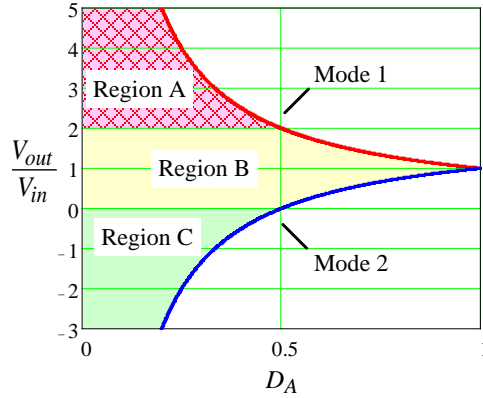


Fig. 13. DC output voltage gain of CF-ZSI and CF-qZSI.

The Z-source inductor current stress of CF-qZSI and CF-ZSI are different according to (2) and (6). Fig. 14 shows the inductor L_1 current stress comparison of the two circuits. It is very clearly, when the open circuit duty cycle D_{op} is changed from $0 \sim 0.5$, which is the motoring mode, the inductor current stress of CF-qZSI is smaller than that of the CF-ZSI. On the other hand, when the open circuit duty cycle D_{op} is changed from $0.5 \sim 1$, which is the regeneration mode, the inductor current stress of CF-qZSI is larger than that of the CF-ZSI. Therefore, CF-qZSI is more suitable working as an inverter for motor drive, and CF-ZSI is more suitable working as a PWM rectifier for generator to charge the battery. This Fig. 14 is a good indication of the inductor current stress. However, when the open circuit duty cycle D_{op} goes to 0.5, the inductor current gain to input current is infinity. That is because when the open circuit duty cycle goes to 0.5, the output voltage is actually zero, so the output power is zero, and the input current I_{in} is also zero accordingly. In this case, any non-zero current through the Z-source inductor will cause the infinity current gain when the open circuit duty cycle is 0.5. This dc analysis only can give us part of the information of inductor current stress, which cannot be used for design.

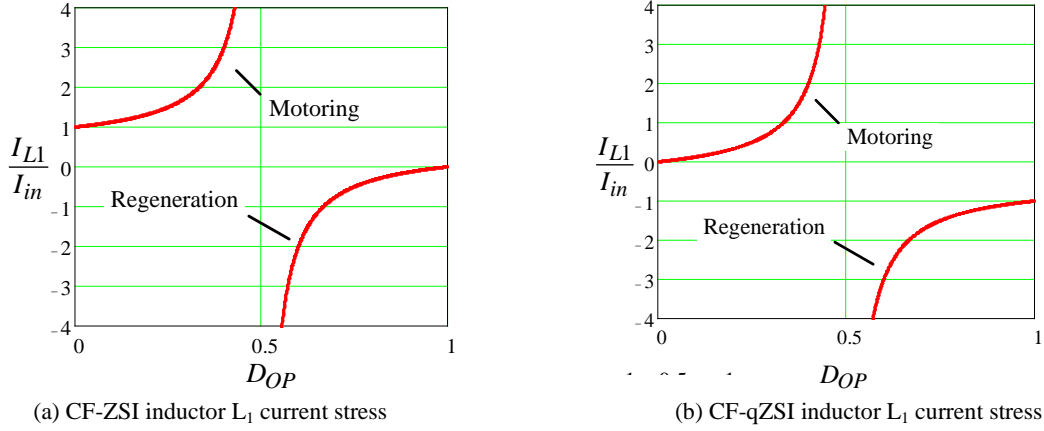


Fig. 14 Inductor L_1 current stress comparison of the two topologies.

Because the CF-ZSI and the CF-qZSI can output lower voltage than the input voltage by inserting open circuit zero state, we can separate the inverter operation to two modes boost mode without any open circuit zero state and buck mode with open circuit zero state. The motor drive also has constant torque and constant power operation region. We can set our CF-Z-source inverter in buck mode operate in the constant torque region, and the boost mode operate in the constant power region. Because during the constant torque region, the output line current will be constant. In the buck mode, the inverter operate in the constant torque region, we can choose the output line current as our base of the current stress to design the Z-source inductors and capacitor.

2. CF-qZSI DC analysis using two switching states with modulation index and power factor

In order to get other insights of the CF-qZSI inverters, we can have other views from dc-link, as shown in Fig. 15. The nine open circuit zero states can be combined into one equivalent circuit, a voltage source can be used to replace the inverter bridge and the load, as shown in Fig. 15(a), and Fig. 15(b) shows the open circuit zero state.

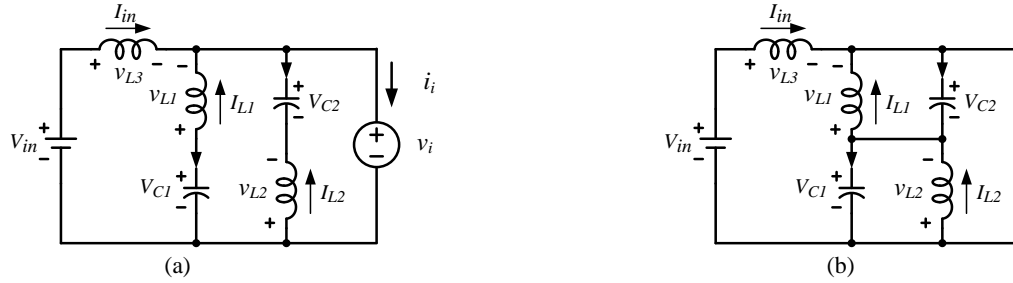


Fig. 15 Equivalent circuit of CF-qZSI viewed from dc-link when the inverter bridge (a) one of the nine non open circuit switching states, (b) open circuit switching state.

For the capacitor C2 we can have the following state equation:

$$i_{C2} = I_{in} + I_{L1} - i_i \quad (9)$$

$$\frac{di_{C2}}{dt} = \frac{1}{C2} (I_{in} + I_{L1} - i_i) \quad (10)$$

Due the circuit symmetry

$$I_{L1} = I_{L2} \quad (11)$$

We can derive that

$$i_i = I_{in} + 2I_{L1} \quad (12)$$

According to (2), we can have that

$$i_i = \frac{1}{1-2D_{op}} I_{in} \quad (13)$$

We can make the current gain as

$$B = \frac{1}{1-2D_{op}} \quad (14)$$

For a current source inverter, if SPWM is used the line peak current i_x (x=a, b, or c) can be written as

$$i_x = M \frac{\sqrt{3}}{2} i_i = BM \frac{\sqrt{3}}{2} I_{in} \quad (15)$$

So the line current rms value can be written as

$$I_{l_rms} = \frac{\sqrt{3}}{2\sqrt{2}} BM I_{in} \quad (16)$$

$$I_{in} = \frac{2\sqrt{2}}{\sqrt{3}} \frac{1}{BM} I_{l_rms} \quad (17)$$

I_{l_rms} is the line current rms value.

According the power balance of input and output, we have

$$V_{in} i_{in} = 3 \frac{v_x}{\sqrt{2}} \frac{i_x}{\sqrt{2}} \cos \delta \quad (18)$$

Plug in (15), we can have

$$\frac{v_x}{V_{in}} = \frac{2i_{in}}{3i_x \cos \delta} = \frac{2}{3} \frac{1}{BM \frac{\sqrt{3}}{2} \cos \delta} = \frac{4}{3\sqrt{3}} \frac{1}{BM \cos \delta} \quad (19)$$

$$v_{ll} = \frac{4}{3} \frac{1}{BM \cos \delta} V_{in} \quad (20)$$

\hat{v}_x is the peak phase voltage, $\cos \delta$ is the power factor, \hat{v}_{ll} is the peak output line voltage. Because the peak line-to-line voltage is smaller than $2V_{in}$, then we can have

$$\sqrt{3}\hat{v}_x = \frac{4}{3\sqrt{3}} \frac{1}{BM \cos \delta} V_{in} \sqrt{3} < 2V_{in} \quad (21)$$

So we will have

$$BM \cos \delta > \frac{2}{3} \quad (22)$$

For three different PWM control method, we can have the different relationship of D_{op} and M .

For the simple boost control:

$$D_{op} = 1 - M \quad (23)$$

$$M = 1 - D_{op} \quad (24)$$

$$B_{simple} = \frac{1}{1 - 2D_{op}} = \frac{1}{2M - 1} \quad (25)$$

$$MB_{simple} = \frac{1 - D_{op}}{1 - 2D_{op}} \quad (26)$$

$$MB_{simple} = \frac{M}{2M - 1} \quad (27)$$

For the constant boost control:

$$D_{op} = 1 - \frac{\sqrt{3}M}{2} \quad (28)$$

$$M = \frac{2}{\sqrt{3}}(1 - D_{op}) \quad (29)$$

$$B_{constant} = \frac{1}{1 - 2D_{op}} = \frac{1}{\sqrt{3}M - 1} \quad (30)$$

$$MB_{constant} = \frac{2}{\sqrt{3}} \frac{1 - D_{op}}{1 - 2D_{op}} \quad (31)$$

$$MB_{constant} = \frac{M}{\sqrt{3}M - 1} \quad (32)$$

For the maximum boost control:

$$D_{op} = \frac{2\pi - 3\sqrt{3}M}{2\pi} \quad (33)$$

$$M = \frac{2\pi}{3\sqrt{3}}(1 - D_{op}) \quad (34)$$

$$B_{maximum} = \frac{\pi}{3\sqrt{3}M - \pi} \quad (35)$$

$$MB_{maximum} = \frac{2\pi}{3\sqrt{3}} \frac{1 - D_{op}}{1 - 2D_{op}} \quad (36)$$

$$MB_{maximum} = \frac{\pi M}{3\sqrt{3}M - \pi} \quad (37)$$

By using the three different, we can revisit the inductor current stress. We already know the inductor current stress in (2) as follows

$$I_{L1} = I_{L2} = \frac{D_{op}}{1 - 2D_{op}} I_{in} \quad (38)$$

Plug in (17), we can have

$$I_{L1} = I_{L2} = \frac{D_{op}}{1 - 2D_{op}} \frac{2\sqrt{2}}{\sqrt{3}} \frac{1}{BM} I_{l_rms} \quad (39)$$

By using three different control methods, we will have different inductor current stress. Plug (26), (31), and (36) into (39), we will have the following results

For simple boost:

$$I_{L1} = I_{L2} = \frac{D_{op}}{1 - D_{op}} \frac{2\sqrt{2}}{\sqrt{3}} I_{l_rms} \quad (40)$$

For constant boost:

$$I_{L1} = I_{L2} = \frac{D_{op}}{1 - D_{op}} \sqrt{2} I_{l_rms} \quad (41)$$

For maximum boost:

$$I_{L1} = I_{L2} = \frac{D_{op}}{1-D_{op}} \frac{3\sqrt{2}}{\pi} I_{l_rms} \quad (42)$$

Fig. 16 shows the normalized Z-source inductor current stress of CF-qZSI in terms of I_{l_rms} , because I_{l_rms} is constant during the whole buck mode. This figure clearly shows that the peak current stress of the Z-source inductor happens when the open circuit duty cycle equals to 0.5. And the peak current stress is about 1.4 times rated load current during the constant torque mode.

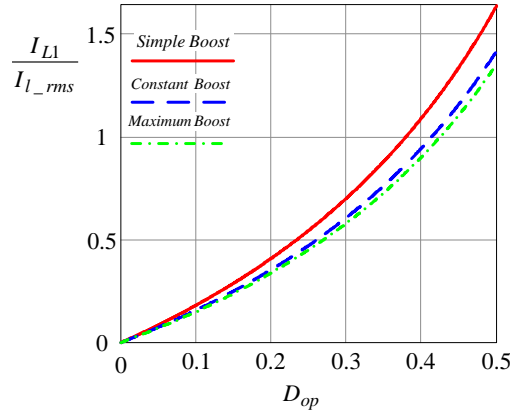


Fig. 16. Normalized Z-source inductor current stress of CF-qZSI in terms of I_{l_rms} .

3. CF-ZSI DC analysis using two switching states with modulation index and power factor

Similarly, we can get the Z-source inductor current stress of CF-ZSI. The two equivalent circuits are shown in Fig. 17.

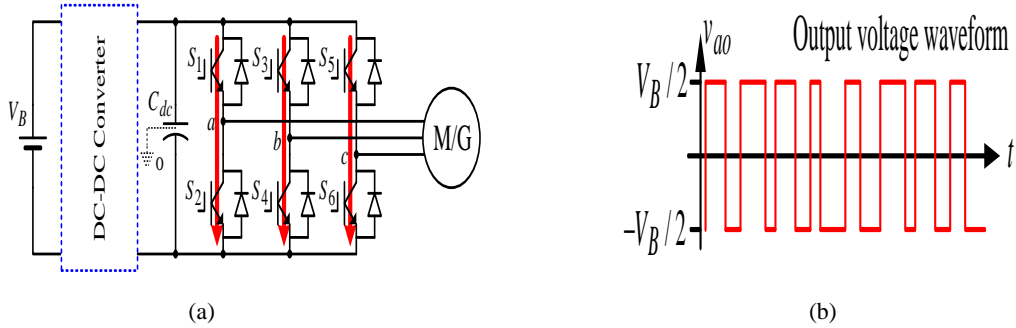


Fig. 17. Equivalent circuit of CF-ZSI viewed from dc-link when the inverter bridge (a) one of the nine non open circuit switching states, (b) open circuit switching state.

For the capacitor C2 we can have the following state equation:

$$\frac{dV_{C2}}{dt} = \frac{1}{C2} (I_{L1} - I_{L2}) \quad (43)$$

$$V_{C2} = \frac{1}{C2} \int (I_{L1} - I_{L2}) dt + V_{C2}(0) \quad (44)$$

Due the circuit symmetry


(45)

We can derive that


(46)

According to (6), we can have that

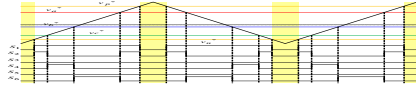

(47)

So the current gain of the CF-ZSI is the same with CF-qZSI, the equations (14) ~ (37) are not needed to derive again.

According to (6) as follows

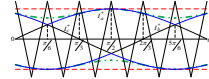

(48)

Plug in (17), we can have


(49)

For different control methods, we can plug (26), (31), and (36) into (49).

For simple boost control

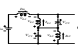

(50)

For constant boost control


(51)

For maximum boost control


(52)

Fig. 18 shows the normalized Z-source inductor current stress of CF-ZSI in terms of . This figure clearly shows that the peak current stress of the Z-source inductor will not change according to the change of open circuit duty cycle. And the current stress is always about 1.4 times rated load current during the constant torque mode. It can be concluded that, the Z-source inductor current stress of CF-ZSI is higher than CF-qZSI during the whole buck mode.

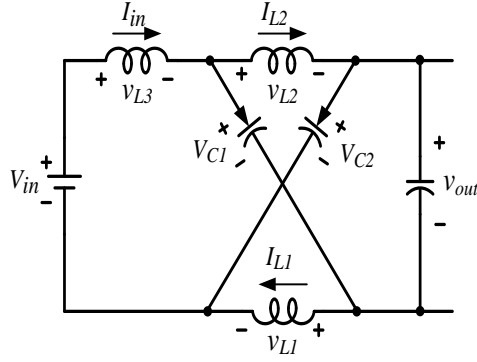



Fig. 18. Normalized Z-source inductor current stress of CF-ZSI in terms of .

Similarly, we can also use the modulation index and the power factor to represent the output current gain and output voltage gain.

b. Current-fed Trans-Z-source and Trans-quasi-Z-source Inverters

1. DC analysis using three switching states with corresponding duty cycle

Fig. 19 shows the equivalent circuits of current-fed trans-Z-source inverter (CF-trans-ZSI) viewed from the dc link. There are three dc operation states, as shown in Fig. 19 (a), (b), and (c). Fig. 19(a) shows the state I, the active state. During this state, the inverter is in one of the six active states, which is equivalent to a dc voltage source. The diode D_1 is not conducting. Fig. 19 (b) shows the state II, the shoot through zero state. During this state, one of the inverter bridges is shorted. The diode D_1 is not conducting. Fig. 19 (c) shows the state III, the open circuit zero state. During this state, all the switches of the inverter are off, and the inverter is equivalent to an open circuit. The diode D_1 is conducting during this state. And Fig. 20 shows the similar three dc equivalent circuits of current-fed trans-quasi-Z-source inverter (CF-trans-qZSI).

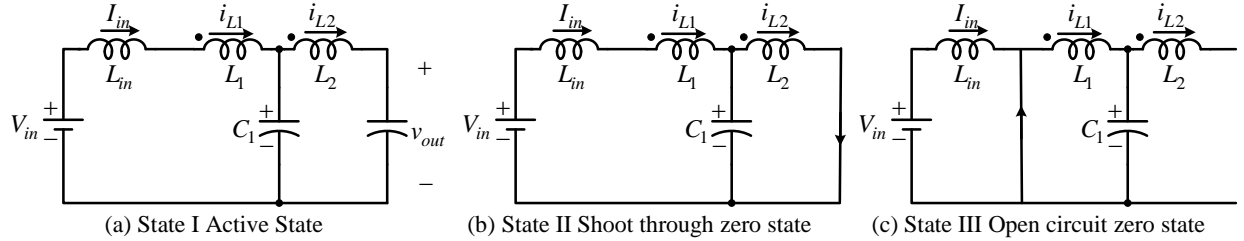


Fig. 19. Equivalent circuit of CF-trans-ZSI.

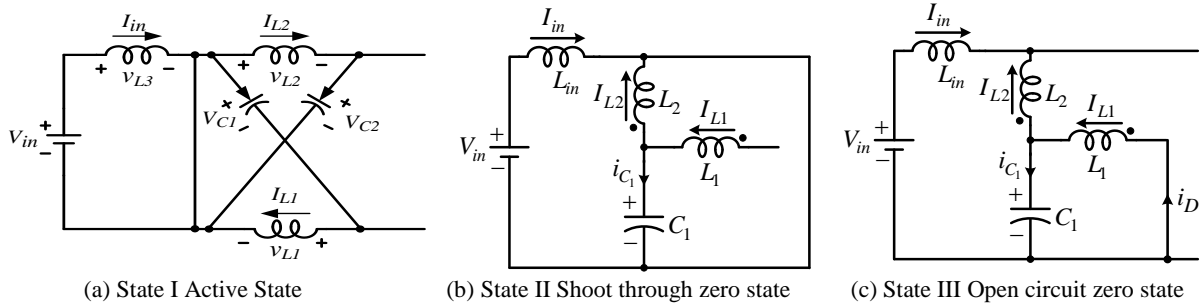


Fig. 20. Equivalent circuit of CF-trans-qZSI.

We first derive the dc steady state equations of CF-trans-ZSI from the equivalent circuits, the following equation is always satisfied:

$$V_{in} - V_{L_{in}} = V_{L_1} + V_{C_1} \quad (53)$$

Because the inductor current during one switching period is zero in steady state, we have

$$V_{in} = V_{C_1} \quad (54)$$

Because inductor L_1 and L_2 is coupled together, and the turns ratio between L_1 and L_2 is $n_1 : n_2$.

So the inductor voltage will be

$$\frac{V_{L_1}}{V_{L_2}} = \frac{n_1}{n_2} \quad (55)$$

When we in active state with the duty cycle is D_A , we have following equations

$$\text{Figure 1: Waveform of } V_{L_1} \text{ and } V_{L_2} \text{ during active state } D_A. \quad (56)$$

$$V_{C_1} = V_{L_2} + V_{out} \quad (57)$$

During duty cycle is equal to D_{sh} we have following equations

$$V_{in} = V_{L_{in}} + V_{L_1} + V_{C_1} \quad (58)$$

$$\text{Figure 2: Waveform of } V_{L_{in}} \text{ during duty cycle } D_{sh}. \quad (59)$$

During the duty cycle equal to D_{op} we have following equations

$$\text{Figure 3: Circuit diagram of CF-trans-ZSI during } D_{op} \text{ state.} \quad (60)$$

$$\text{Figure 4: Circuit diagram of CF-trans-ZSI during } D_{sh} \text{ state.} \quad (61)$$

According to input inductor L_{in} state balance equation

$$V_{L_{in}} D_A + V_{L_{in}} D_{sh} + V_{L_{in}} D_{op} = 0 \quad (62)$$

Plug equation (53)-(61) into (62) we have

$$-\frac{n_1}{n_2} (V_{in} - V_{out}) D_A + \frac{n_1}{n_2} (-V_{in}) D_{sh} + V_{in} D_{op} = 0 \quad (63)$$

So the voltage gain of CF-trans-ZSI is

$$\frac{V_{out}}{V_{in}} = \frac{1 - D_{op}(1 + \frac{n_2}{n_1})}{D_A} \quad (64)$$

$$\frac{V_{out}}{V_{in}} = \begin{cases} \frac{1}{D_A} & \text{if } D_{op} = 0 \\ \frac{3D_A - 2}{D_A} & \text{if } D_{sh} = 0 \end{cases} \quad (65)$$

Similarly, the dc voltage gain of CF-trans-qZSI can be also derived. The result is the same with the CF-trans-ZSI as shown in (64) and (65). Fig. 21 shows the dc output voltage gain of CF-trans-ZSI and CF-trans qZSI. For both of the two topologies, there are three different operation regions. Region B is the motoring region, the inverter equivalent dc output voltage is between $0 \sim 3V_{in}$. Region C is the regenerative region, because the output voltage gain is negative. In this region, the inverter can operate as a PWM rectifier to charge the input battery. Region A is the prohibited region, if the output voltage gain is larger than three, the diode of the Z-source network will conduct automatically. The output voltage will get distortion due to the unwanted conduction of the diode. If we want to extend the motoring operation region of these two circuits, a reverse blocking switching device will have to be added to replace the diode. Mode 1 is the motoring operation region line without any open circuit zero states, where the highest voltage gain can be achieved. Mode 2 is the regeneration region line where all the shoot through zero states are replaced by the open circuit zero state. During this mode, these two inverters can output the lowest possible voltage. It can be derived from the comparison of Fig. 13 and Fig. 21, the motoring region of the CF-trans-ZSI and CF-trans-qZSI are extended. The maximum output voltage gain is three times of the input voltage. So by changing the transformer turns ration of CF-trans-ZSI and CF-trans-qZSI, the motoring operation region can be extended without adding extra active switch.

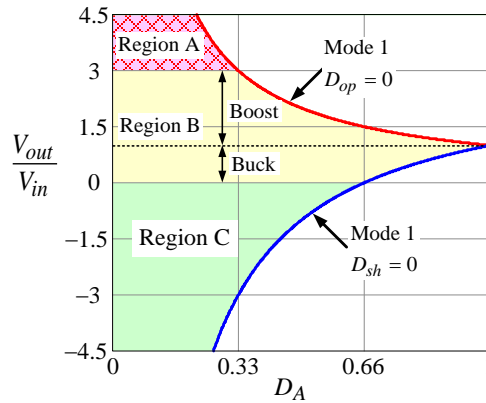


Fig. 21. DC output voltage gain of CF-trans-ZSI and CF-trans-qZSI.

2. CF-trans-ZSI DC analysis using two switching states with modulation index and power factor

Fig. 22 shows the equivalent circuit of the CF-trans-ZSI viewed from the dc-link.

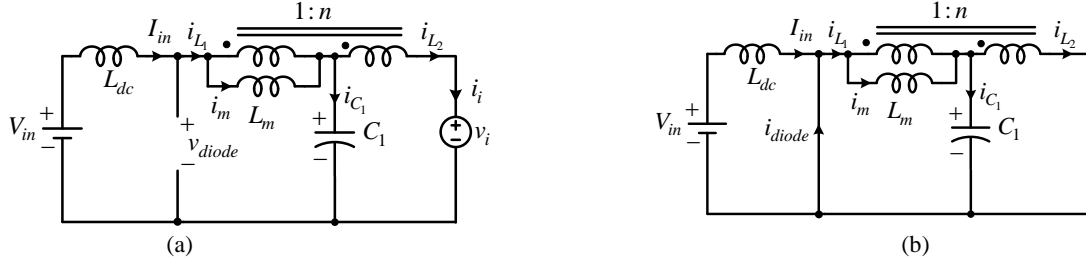


Fig. 22. Equivalent circuit of the CF-trans-Z-source inverter viewed from the dc link when the inverter bridge (a) one of the nine nonopen-circuit switching states (b) open-circuit switching state.

When the circuit is at non-open-circuit switching state with conduction time equals to $(1 - D_{op})T_S$, we have the following equation:

$$I_{in} = i_{L1} \quad (66)$$

$$i_{L1} = i_C + i_{L2} \quad (67)$$

$$i_{L2} = i_i \quad (68)$$

When the circuit is at open-circuit switching state, with conduction time equals to $D_{op}T_S$ we have the following equation:

$$i_{in} + i_D = i_{L1} \quad (69)$$

$$i_{L1} = i_{C1} \quad (70)$$

$$i_i = 0 \quad (71)$$

$$i_D = ni_{L2} = ni_i \quad (72)$$

It looks like the inductor current i_{L2} should be zero but it suppose to have current, and it was forced to transfer his current to the diode, so the diode current should be the old inductor L_2 current which is force to the primary side.

Due to the capacitor current charging balance, and plug the (66)-(72) we have the following equation:

$$(I_{in} - i_i)(1 - D_{op}) + (I_{in} + ni_i)D_{op} = 0 \quad (73)$$

$$i_i = \frac{1}{1 - D_{op} - nD_{op}} I_{in} \quad (74)$$

$$B = \frac{1}{1 - (n+1)D_{op}} \quad (75)$$

For three different PWM control method, we can have the different relationship of D_{op} and M .

For the simple boost control:

$$D_{op} = 1 - M \quad (76)$$

$$M = 1 - D_{op} \quad (77)$$

$$B_{simple} = \frac{1}{1 - (n+1)D_{op}} = \frac{1}{(n+1)M - n} \quad (78)$$

$$MB_{simple} = \frac{1 - D_{op}}{1 - (n+1)D_{op}} \quad (79)$$

$$MB_{simple} = \frac{M}{(n+1)M - n} \quad (80)$$

For the constant boost control:

$$D_{op} = 1 - \frac{\sqrt{3}M}{2} \quad (81)$$

$$M = \frac{2}{\sqrt{3}}(1 - D_{op}) \quad (82)$$

$$B_{constant} = \frac{1}{1 - (n+1)D_{op}} = \frac{1}{\frac{\sqrt{3}}{2}(n+1)M - n} \quad (83)$$

$$MB_{constant} = \frac{2}{\sqrt{3}} \frac{1 - D_{op}}{1 - (n+1)D_{op}} \quad (84)$$

$$MB_{constant} = \frac{M}{\frac{\sqrt{3}}{2}(n+1)M - n} \quad (85)$$

For the maximum boost control:

$$D_{op} = \frac{2\pi - 3\sqrt{3}M}{2\pi} \quad (86)$$

$$M = \frac{2\pi}{3\sqrt{3}}(1 - D_{op}) \quad (87)$$

$$B_{maximum} = \frac{1}{1 - (n+1)D_{op}} = \frac{1}{\frac{3\sqrt{3}}{2\pi}(n+1)M - n} \quad (88)$$

$$MB_{maximum} = \frac{2\pi}{3\sqrt{3}} \frac{1 - D_{op}}{1 - (n+1)D_{op}} \quad (89)$$

$$MB_{maximum} = \frac{M}{\frac{3\sqrt{3}}{2\pi} (n+1)M - n} \quad (90)$$

The CF-trans-qZSI dc steady state equation is same with the CF-trans-ZSI, which will not be derived here. The inductor current stress of CF-trans-qZSI and CF-trans-ZSI is different, which will be discussed in detail in the passive components design section.

Because we already derived that

$$V_{ll} = \frac{4}{3} \frac{1}{BM \cos \delta} V_{in} \quad (91)$$

By plugging (80), (85), (90) into it, we can derive the output line-to-line voltage gain in terms of input voltage.

Table I shows the open circuit duty cycle, the voltage gain and current gain corresponding to modulation index of three different control strategies. When $n=1$ the table also can represent the situation of CF- ZSI/qZSI.

Table I Comparison of three different control strategies

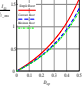
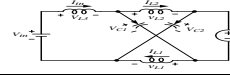
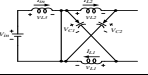
	D_{op} values due to M	Voltage gain $\frac{V_{ll}}{V_{dc}}$	Current gain 
Simple boost	$1 - M$		
Maximum boost	$1 - \frac{3\sqrt{3}M}{2\pi}$	$\frac{4}{3M \cos \delta} \left(\frac{3\sqrt{3}M}{2\pi} (1+n) - n \right)$	$\frac{2\pi M}{3\sqrt{3}M(n+1) - 2\pi n}$
Constant boost	$1 - \frac{\sqrt{3}M}{2}$	$\frac{4}{3M \cos \delta} \left(\frac{\sqrt{3}M}{2} (1+n) - n \right)$	$\frac{2M}{\sqrt{3}M(n+1) - 2n}$

Fig. 23 shows the output line-to-line peak voltage gain of CF-trans-ZSI and CF-trans-qZSI in terms of modulation index and assuming power factor equals to 1.

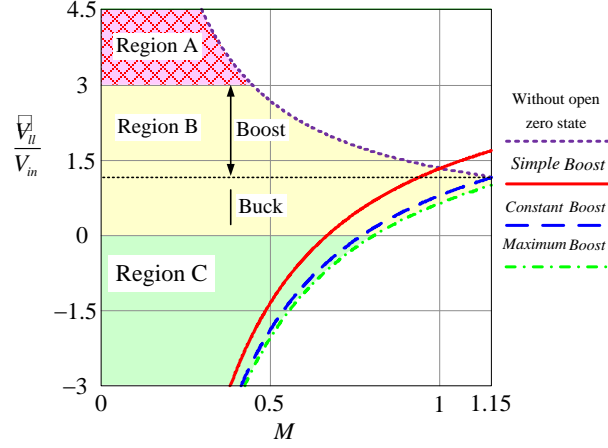


Fig. 23. Output voltage gain curve of CF-trans-ZSI and CF-trans-qZSI with three different control methods when $n=2$.

2. Total Device Stress Ratio

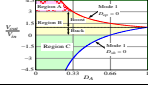
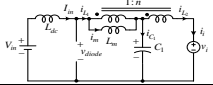
a. TSDPSR of the four topologies using P_o as the power base in terms of D_{op} :

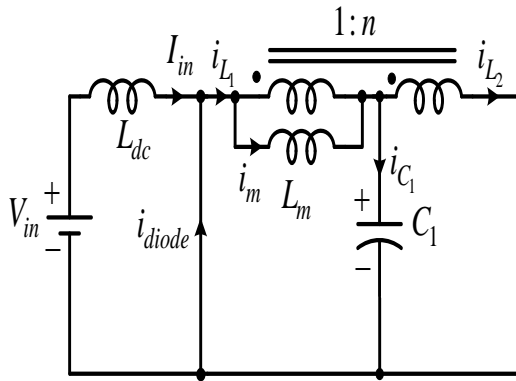
In the inverter system, each switching device should be chosen according to the maximum voltage across the device and the peak and average current through it. To qualify the voltage and current stress of the inverter and compare different topologies, the total switching device power stress ratio (TSDPSR) can be introduced. The TSDPSR of an inverter system can be used to evaluate different topologies in terms of cost. The definitions are summarized as follows:

$$\text{TSDPSR}_{average} = \sum_{m=1}^N V_m I_{m_average} / P_o \quad \text{and} \quad \text{TSDPSR}_{peak} = \sum_{m=1}^N V_m I_{m_peak} / P_o$$

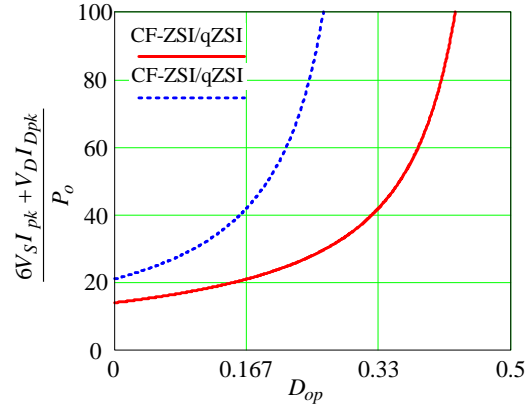
Where N is the total device number in the inverter system, V_m is the peak voltage across the device, $I_{m_average}$ and I_{m_peak} are the average and peak current through the device. In the following comparison, the diode voltage and current stress are also considered as part of the average TSDPSR and peak TSDPSR. Assume maximum boost control is used for the CF-ZSI and CF-qZSI. P_o is the peak output power, V_{in} is the input voltage at the peak output power. V_{in_peak} is the peak input voltage. The switching device stress comparison is summarized in Table II.

Table II Switching device stress comparison of CF-PI, CF-ZSI/qZSI and CF-trans-ZSI/qZSI

	CF-ZSI/qZSI	CF-trans-ZSI/qZSI
Switching device voltage stress V_S	$2V_{max}$	$(n+1)V_{max}$
Diode voltage stress V_D	$2V_{max}$	$\left(1+\frac{1}{n}\right)V_{max}$
Switch average current stress I_{ave}	$\frac{1-D_{op}}{3(1-2D_{op})} \frac{P_o}{V_i}$	$\frac{1-D_{op}}{3(1-(n+1)D_{op})} \frac{P_o}{V_i}$
Diode average current stress I_D	$\frac{D_{op}}{1-2D_{op}} \frac{P_o}{V_i}$	$\frac{nD_{op}}{1-(n+1)D_{op}} \frac{P_o}{V_i}$
Average TSDPSR $(6V_S I_{ave} + V_D I_D)/P_o$	$\frac{2(2-D_{op})V_{max}}{(1-2D_{op})V_i}$	$\frac{(n+1)(2-D_{op})V_{max}}{(1-(n+1)D_{op})V_i}$
Switching peak current stress I_{pk}	$\frac{1}{1-2D_{op}} \frac{P_o}{V_i}$	$\frac{1}{1-(n+1)D_{op}} \frac{P_o}{V_i}$
Diode peak current stress I_{Dpk}	$\frac{1}{1-2D_{op}} \frac{P_o}{V_i}$	$\frac{n}{1-(n+1)D_{op}} \frac{P_o}{V_i}$
Peak TSDPSR $(6V_S I_{pk} + V_D I_{Dpk})/P_o$		



(a) Average TSDPSR



(b) Peak TSDPSR

Fig. 24. Average TSDPSR and Peak TSDPSR of the four topologies.

b. TSDPSR of the four topologies using $V_{max} I_{l_rms}$ as the power base in terms of M:

Fig. 24 shows the average TSDPSR and peak TSDPSR of the four topologies in terms of open circuit zero state. But because the input current is zero at 0.5 open circuit duty cycle for CF-ZSI/qZSI or 0.333 for CF-trans-ZSI/qZSI, we have the infinity total device stress which is unreasonable similar to the current gain. We need to use the output line current to replace the input current to get the finite value. Table III shows the switching device stress comparison using the modulation index and power factor. The line current is used as the base for the power. Because buck mode using maximum boost control and the boost mode are not continuous, as shown in Fig. 23. We use the constant boost control to calculate the TSDPSR.

Table III Switching device stress comparison of CF-PI, CF-ZSI/qZSI and CF-trans-ZSI/qZSI using M and $\cos\delta$

	CF-ZSI/qZSI	CF-trans-ZSI/qZSI
Switching device voltage stress V_S	$2V_{max}$	$(n+1)V_{max}$
Diode voltage stress V_D	$2V_{max}$	$\left(1+\frac{1}{n}\right)V_{max}$
Switch average current stress I_{ave}	$\frac{\sqrt{2}}{3}I_{l_rms}$	$\frac{\sqrt{2}}{3}I_{l_rms}$
Diode average current stress I_D	$\frac{\sqrt{2}(2-\sqrt{3}M)}{\sqrt{3}M}I_{l_rms}$	$\frac{\sqrt{2}n(2-\sqrt{3}M)}{\sqrt{3}M}I_{l_rms}$
Average TSDPSR $(6V_S I_{ave} + V_D I_D)/V_{max} I_{l_rms}$	$4\sqrt{2} + \frac{2\sqrt{2}(2-\sqrt{3}M)}{\sqrt{3}M}$	$4\sqrt{2} + \frac{2\sqrt{2}n(2-\sqrt{3}M)}{\sqrt{3}M}$
Switching peak current stress I_{pk}	$\frac{2\sqrt{2}}{\sqrt{3}} \frac{1}{M} I_{l_rms}$	$\frac{2\sqrt{2}}{\sqrt{3}} \frac{1}{M} I_{l_rms}$
Diode peak current stress I_{Dpk}	$\frac{2\sqrt{2}}{\sqrt{3}} \frac{1}{M} I_{l_rms}$	$\frac{2\sqrt{2}}{\sqrt{3}} \frac{n}{M} I_{l_rms}$
Peak TSDPSR $(6V_S I_{pk} + V_D I_{Dpk})/V_{max} I_{l_rms}$	$\frac{28\sqrt{2}}{\sqrt{3}M}$	$\frac{24\sqrt{2} + 4\sqrt{2}n}{\sqrt{3}M}$

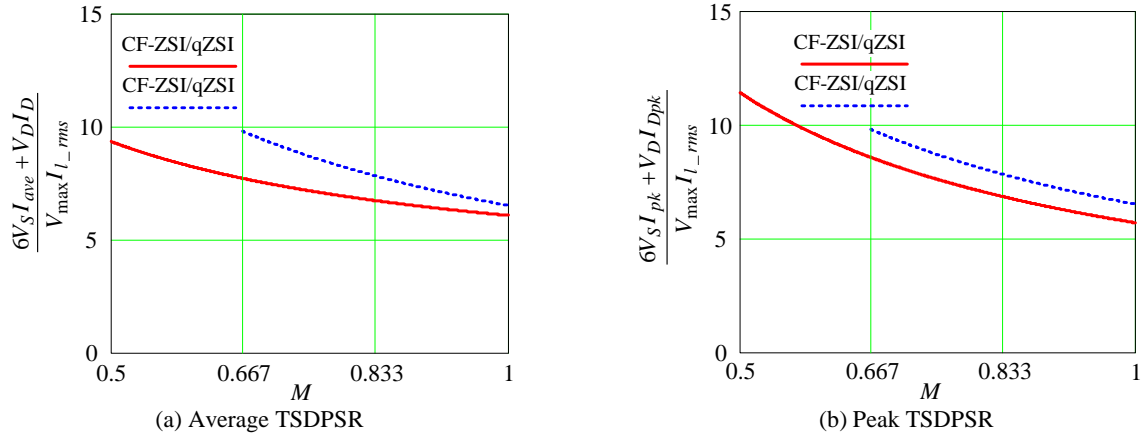
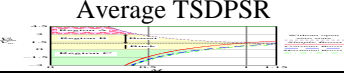


Fig. 25. Average TSDPSR and Peak TSDPSR of the four topologies.

c. **TSDPSR of the four Topologies Using $V_{max} I_{l_rms}$ as the power base in terms of D_{op}**

In the similar way, by changing the power base to $V_{max} I_{l_rms}$, we can also get the TSDPSR in terms of D_{op} as shown in Table IV.

Table IV Switching device stress comparison of CF-PI, CF-ZSI/qZSI and CF-trans-ZSI/qZSI using $V_{\max} I_{l_rms}$ as power base

	CF-ZSI/qZSI	CF-trans-ZSI/qZSI
Switching device voltage stress V_S	$2V_{\max}$	$(n+1)V_{\max}$
Diode voltage stress V_D	$2V_{\max}$	$\left(1+\frac{1}{n}\right)V_{\max}$
Switch average current stress I_{ave}	$\frac{\sqrt{2}}{3} I_{l_rms}$	$\frac{\sqrt{2}}{3} I_{l_rms}$
Diode average current stress I_D	$\frac{\sqrt{2}D_{op}}{1-D_{op}} I_{l_rms}$	$\frac{\sqrt{2}nD_{op}}{1-D_{op}} I_{l_rms}$
 Average TSDPSR	$4\sqrt{2} + \frac{2\sqrt{2}D_{op}}{1-D_{op}}$	$2\sqrt{2}(n+1) + \frac{\sqrt{2}D_{op}}{1-D_{op}}(1+n)$
Switching peak current stress I_{pk}	$\frac{\sqrt{2}}{1-D_{op}} I_{l_rms}$	$\frac{\sqrt{2}}{1-D_{op}} I_{l_rms}$
Diode peak current stress I_{Dpk}	$\frac{\sqrt{2}}{1-D_{op}} I_{l_rms}$	$\frac{\sqrt{2}n}{1-D_{op}} I_{l_rms}$
Peak TSDPSR $(6V_S I_{pk} + V_D I_{Dpk}) / V_{\max} I_{l_rms}$	$\frac{14\sqrt{2}}{(1-D_{op})}$	$\frac{7\sqrt{2}(n+1)}{1-D_{op}}$

In conclusion, the switching device stresses of CF-ZSI and CF-qZSI are the same, the switching device stresses of CF-trans-ZSI and CF-trans-qZSI are also the same. By using transformer, the CF-trans-ZSI/qZSI can increase the output voltage boost ratio in motoring region. At the same time the voltage stress of the device is also increased. Although the diode voltage stress will decrease with the increase of transformer turns ratio, the diode peak current will increase according to it. The increased turn off current of the diode may cause more sever voltage overshoot across it.

3. Passive Components Design

a. Current-fed Quasi-Z-source Inverter (CF-qZSI)

1. Z-source Capacitor

a. Capacitor Voltage Stress

The capacitor is in dc side, the inductor voltage under steady state is zero, so the voltage stress of both Z-source capacitors is V_{in} .

b. Capacitor Current Stress

The Z-source capacitor current is near zero during the non-open zero state operation. So we only consider the capacitor current stress in buck/constant torque mode.

The capacitor current is $I_{in} + I_{L1}$ during the open zero state, and the capacitor current is $-I_{L1}$ during other states.

The capacitor RMS current is

$$I_{C_rms} = \sqrt{D_{op}(I_{in} + I_{L1})^2 + (1 - D_{op})(-I_{L1})^2} \quad (92)$$

And the inductor current is

$$I_{L1} = I_{L2} = \frac{D_{op}}{1 - 2D_{op}} I_{in} \quad (93)$$

So, by plugging (93) into (92), we can get

$$I_{C_rms} = \frac{I_{in}}{1 - 2D_{op}} \sqrt{D_{op}(1 - D_{op})} \quad (94)$$

Because we already know that

$$I_{in_peak} = \frac{2\sqrt{2}I_{l_rms}}{\sqrt{3}BM} \quad (95)$$

So we can plug (95) into (94) and get

$$I_{C_rms} = \frac{2\sqrt{2}I_{l_rms}}{\sqrt{3}BM(1 - 2D_{op})} \sqrt{D_{op}(1 - D_{op})} \quad (96)$$

By plug in the relationship of BM in three different control methods (23)~(37), we can get, simple boost control:

$$I_{C_rms} = \frac{2\sqrt{2}I_{l_rms}}{\sqrt{3}} \sqrt{\frac{(1 - M)}{M}} \quad (97)$$

$$I_{C_rms} = \frac{2\sqrt{2}I_{l_rms}}{\sqrt{3}} \sqrt{\frac{D_{op}}{(1 - D_{op})}} \quad (98)$$

Constant boost control:

$$I_{C_rms} = \frac{2\sqrt{2}I_{l_rms}}{\sqrt{3}} \sqrt{\left(1 - \frac{\sqrt{3}M}{2}\right) \frac{\sqrt{3}}{2M}} \quad (99)$$

$$I_{C_rms} = \sqrt{2}I_{l_rms} \sqrt{\frac{D_{op}}{(1 - D_{op})}} \quad (100)$$

Maximum boost control:

$$I_{C_rms} = \frac{2\sqrt{2}I_{l_rms}}{\sqrt{3}} \sqrt{\left(1 - \frac{3\sqrt{3}M}{2\pi}\right) \frac{3\sqrt{3}}{2\pi M}} \quad (101)$$

$$I_{C_rms} = \frac{3\sqrt{2}I_{l_rms}}{\pi} \sqrt{\frac{D_{op}}{(1-D_{op})}} \quad (102)$$

Fig. 26 shows the normalized capacitor current stresses with three different control methods using I_{l_rms} as the base current.

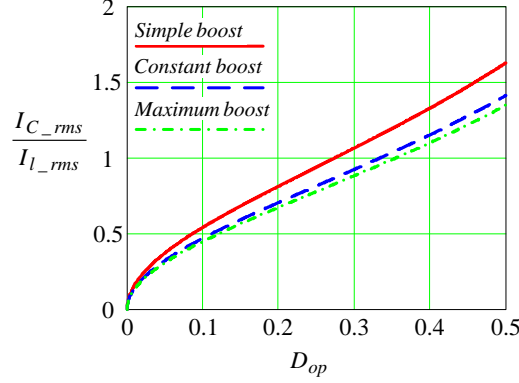


Fig. 26. The normalized capacitor current stresses with three control methods.

c. Capacitance

Assume the capacitor ripple to be 10%.

Because the capacitor voltage is equal to the input voltage, so the capacitor ripple is

$$\Delta V_C = 10\% V_{in} \quad (103)$$

Simple boost control:

$$C = \frac{(I_{in} + I_{L1})D_{op}T_S}{\Delta V_C} = \frac{D_{op} 2\sqrt{2}I_{l_rms}T_S}{10\%\sqrt{3}V_{in}} \quad (104)$$

Constant boost control:

$$C = \frac{(I_{in} + I_{L1})D_{op}T_S}{\Delta V_C} = \frac{D_{op}\sqrt{2}I_{l_rms}T_S}{10\%V_{in}} \quad (105)$$

Maximum boost control:

$$C = \frac{(I_{in} + I_{L1})D_{op}T_S}{\Delta V_C} = \frac{D_{op} 3\sqrt{2}I_{l_rms}T_S}{10\%\pi V_{in}} \quad (106)$$

Assume the base is

$$\frac{I_{l_rms}T_S}{2\pi V_{in}} \quad (107)$$

Fig. 27 shows the normalized capacitance requirement with three control methods.

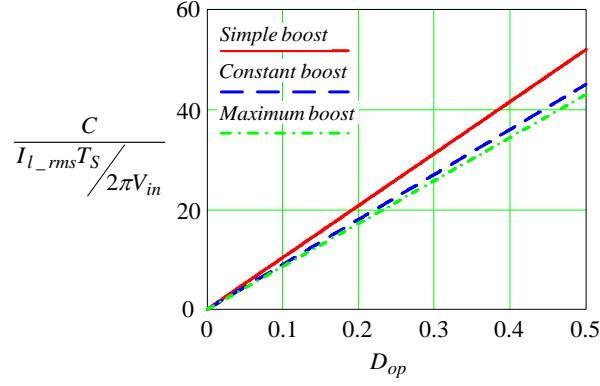


Fig. 27. Capacitance requirement comparison with three control methods.

2. Z-source Inductor

a. Inductor Current Stress

Because we already derive this part in DC analysis and operation region section, we just put the results here.

Simple boost:

$$I_{L1} = I_{L2} = \frac{D_{op}}{1-D_{op}} \frac{2\sqrt{2}I_{l_rms}}{\sqrt{3}} \quad (108)$$

Constant boost:

(109)

Maximum boost:

(110)

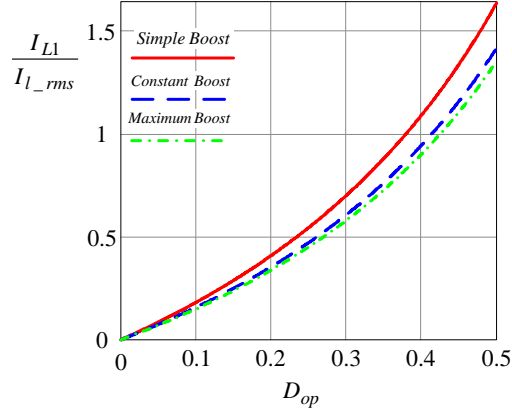


Fig. 28. Normalized Z-source inductor current stress of CF-qZSI in terms of I_{l_rms} .

b. Inductance

Assume the inductor current ripple is about 30% of the inductor dc current

Z-source inductor:

$$L_1 = \frac{V_{in} D_{op} T_S}{30\% I_{L1}} \quad (111)$$

By plugging in (40) (41) (42) into (111) we can get the inductance requirement of three control method.

Simple boost:

$$L_1 = \frac{V_{in} D_{op} T_S}{30\% I_{L1}} = \frac{V_{in} T_S (1 - D_{op}) \sqrt{3}}{30\% 2\sqrt{2} I_{l_rms}} \quad (112)$$

Constant boost:

$$L_1 = \frac{V_{in} D_{op} T_S}{30\% I_{L1}} = \frac{V_{in} T_S (1 - D_{op})}{30\% \sqrt{2} I_{l_rms}} \quad (113)$$

Maximum boost:

$$L_1 = \frac{V_{in} D_{op} T_S}{30\% I_{L1}} = \frac{V_{in} T_S (1 - D_{op}) \pi}{30\% 3\sqrt{2} I_{l_rms}} \quad (114)$$

Assume the base is

$$\frac{V_{in} T_S}{2\pi I_{l_rms}} \quad (115)$$

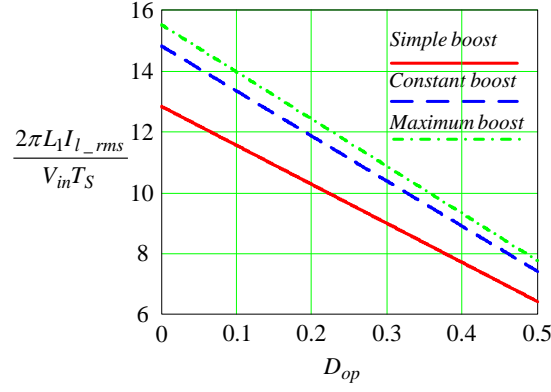


Fig. 29. Normalized Z-source inductor inductance of CF-qZSI with three control methods.

3. Input Inductor

a. Inductor Current Stress

The input inductor current stress is also derived in (17), we just put the result here.

$$I_{in_peak} = \frac{2\sqrt{2}I_{l_rms}}{\sqrt{3}BM} \quad (116)$$

Simple boost:

$$I_{in_peak} = \frac{2\sqrt{2}I_{l_rms}}{\sqrt{3}} \frac{1-2D_{op}}{1-D_{op}} \quad (117)$$

Constant boost:

$$I_{in_peak} = \sqrt{2}I_{l_rms} \frac{1-2D_{op}}{1-D_{op}} \quad (118)$$

Maximum boost:

$$I_{in_peak} = \frac{3\sqrt{2}I_{l_rms}}{\pi} \frac{1-2D_{op}}{1-D_{op}} \quad (119)$$

Fig. 30 shows the normalized inductor current stresses with three different control methods.

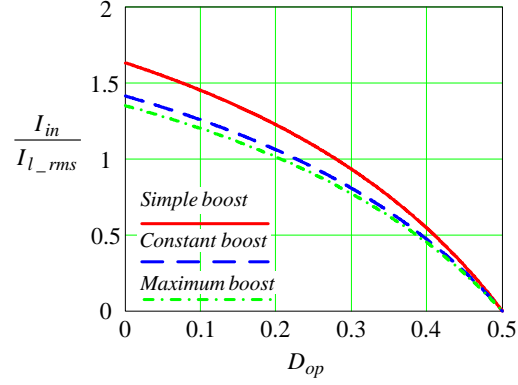


Fig. 30 Normalized input inductor current stresses with three control methods.

b. Inductance

If the open zero state existed, the inductance can be calculated as follows:

$$L_{in} = \frac{V_{in} D_{op} T_S}{30\% I_{in}} \quad (120)$$

Plug (17) into (120) we can get

$$L_{in} = \frac{V_{in} D_{op} T_S \sqrt{3} B M}{30\% 2 \sqrt{2} I_{l_rms}} \quad (121)$$

Plug (40) (41) (42) into the equation ,we can get

Simple boost

$$L_{in} = \frac{V_{in} D_{op} T_S \sqrt{3} (1 - D_{op})}{30\% 2 \sqrt{2} I_{l_rms} (1 - 2 D_{op})} \quad (122)$$

Constant boost:

$$L_{in} = \frac{V_{in} D_{op} T_S (1 - D_{op})}{30\% \sqrt{2} I_{l_rms} (1 - 2 D_{op})} \quad (123)$$

Maximum boost:

$$L_{in} = \frac{V_{in} D_{op} T_S \pi (1 - D_{op})}{30\% 3 \sqrt{2} I_{l_rms} (1 - 2 D_{op})} \quad (124)$$

Assume the base is:

$$\frac{V_{in} T_S}{2\pi I_{l_rms}} \quad (125)$$

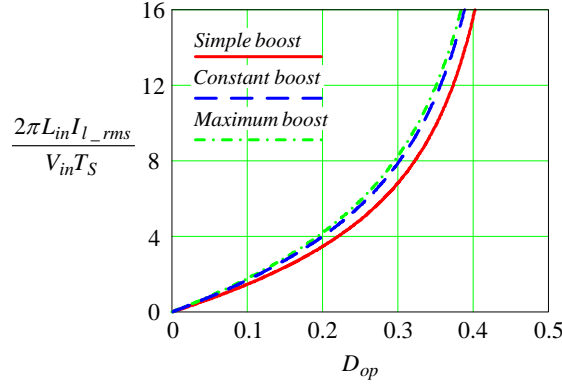


Fig. 31. Normalized inductance of input inductor with three control methods.

b. Current-fed Z-source Inverter (CF-ZSI)

1. Z-source Capacitor

a. Capacitor Voltage Stress

The capacitor is in dc side, the inductor voltage under steady state is zero, so the voltage stress of both Z-source capacitors is V_{in} .

b. Capacitor Current Stress

The Z-source capacitor current is near zero during the non-open zero state operation.

The capacitor C2 current is I_{L1} during the open zero state, and the capacitor current is $I_{in} - I_{L2}$ during other states, because the inductor current is large than the input current, $I_{in} - I_{L2}$ is a negative value.

And the capacitor RMS current is

$$I_{C_rms} = \sqrt{D_{op} I_{L1}^2 + (1 - D_{op})(I_{in} - I_{L2})^2} \quad (126)$$

Because

$$I_{L1} = I_{L2} = \frac{1 - D_{op}}{1 - 2D_{op}} I_{in} \quad (127)$$

So plug (127) into (126) we can get

$$I_{C_rms} = \frac{I_{in}}{1 - 2D_{op}} \sqrt{D_{op}(1 - D_{op})} \quad (128)$$

Because the output rated line current is constant during the buck/constant torque mode, so we should choose the output line current as the base to determine the required rms current for the capacitor.

Since we already know:



The capacitor rms current can be indicated by rated line current as follows:

$$I_{C_rms} = \frac{2\sqrt{2}}{\sqrt{3}} \frac{\sqrt{D_{op}(1-D_{op})}}{BM(1-2D_{op})} I_{l_rms} \quad (130)$$

So the capacitor current stress for CF-ZSI is the same with the quasi-Z-source because they share the same BM.

Simple boost

$$I_{C_rms_simple} = \frac{2\sqrt{2}}{\sqrt{3}} \sqrt{\frac{D_{op}}{(1-D_{op})}} I_{l_rms} \quad (131)$$

Constant boost

$$I_{C_rms_constant} = \sqrt{2} \sqrt{\frac{D_{op}}{(1-D_{op})}} I_{l_rms} \quad (132)$$

Maximum boost

$$I_{C_rms_simple} = \frac{3\sqrt{2}}{\pi} \sqrt{\frac{D_{op}}{(1-D_{op})}} I_{l_rms} \quad (133)$$

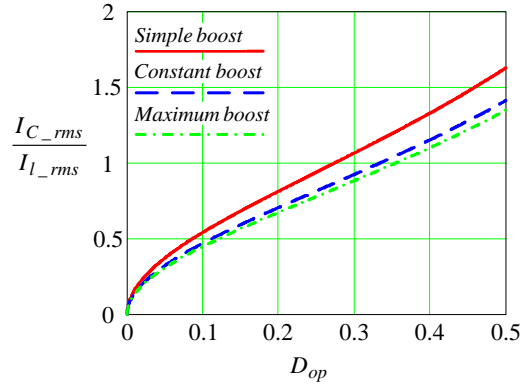


Fig. 32. The normalized capacitor current stresses with three control methods.

c. Capacitance

$$C = \frac{I_{L1}D_{op}T_S}{\Delta V_C} = \frac{(1-D_{op})D_{op}}{1-2D_{op}} \frac{1}{BM} \frac{2\sqrt{2}I_{l_rms}T_S}{\sqrt{3} \cdot 10\%V_{in}} \quad (134)$$

Plug in the BM of three method. We can get:

Simple boost

$$C_{simple} = D_{op} \frac{2\sqrt{2}I_{l_rms}T_S}{\sqrt{3} \cdot 10\%V_{in}} \quad (135)$$

Constant boost:

$$C_{constant} = D_{op} \frac{\sqrt{2}I_{l_rms}T_S}{10\%V_{in}} \quad (136)$$

Maximum boost:

$$C_{maximum} = D_{op} \frac{3\sqrt{2}I_{l_rms}T_S}{\pi \cdot 10\%V_{in}} \quad (137)$$

Assume the base is

$$\frac{I_{l_rms}T_S}{2\pi V_{in}} \quad (138)$$

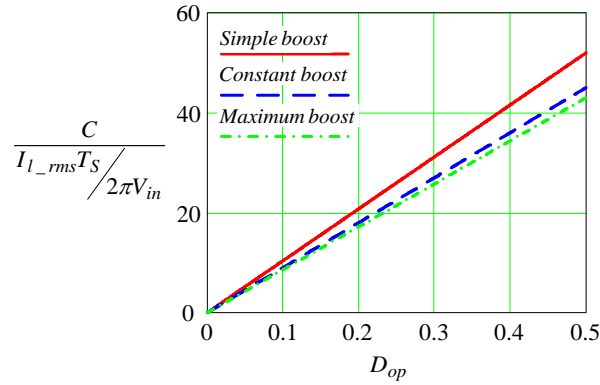


Fig. 33. Capacitance requirement comparison with three control methods

2. Z-source Inductor

a. Inductor Current Stress

The Z-source inductor current stress have been derived previously, we just put the results here.

Simple boost:

$$I_{L1} = I_{L2} = \frac{2\sqrt{2}}{\sqrt{3}} I_{l_rms} \quad (139)$$

Constant boost:

$$I_{L1} = I_{L2} = \sqrt{2}I_{l_rms} \quad (140)$$

Maximum boost:

$$I_{L1} = I_{L2} = \frac{3\sqrt{2}}{\pi}I_{l_rms} \quad (141)$$

Fig. 34 shows the CF-ZSI Z-source inductor current stress with three different control methods. Fig. 35 shows the Z-source inductor current stress comparison of CF-ZSI and CF-qZSI with three different control methods.

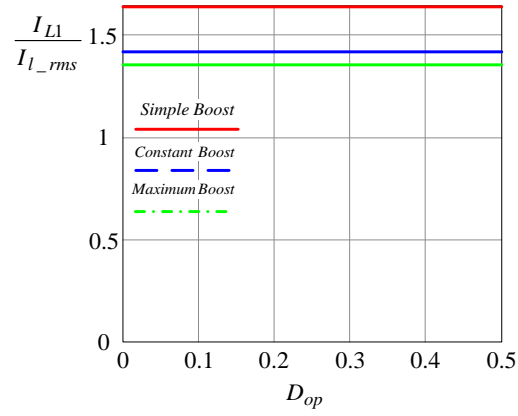


Fig. 34 Inductor current stress of three control methods.

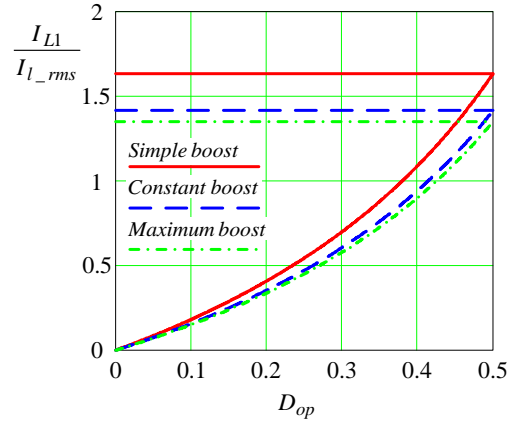


Fig. 35. Inductor current stress comparison of CF-ZSI and CF-qZSI with three control methods.

b. Inductance

Z-source inductor:

$$L_1 = \frac{V_{in}D_{op}T_S}{\Delta I} = \frac{V_{in}D_{op}T_S}{30\%I_{L1}} \quad (142)$$

Plug in the I_{L1} of three control methods.

$$L_{1_simple} = D_{op} \frac{\sqrt{3}V_{in}T_S}{30\%2\sqrt{2}I_{l_rms}} \quad (143)$$

$$L_{1_constant} = D_{op} \frac{V_{in}T_S}{30\%\sqrt{2}I_{l_rms}} \quad (144)$$

$$L_{1_maximum} = D_{op} \frac{\pi V_{in}T_S}{30\%3\sqrt{2}I_{l_rms}} \quad (145)$$

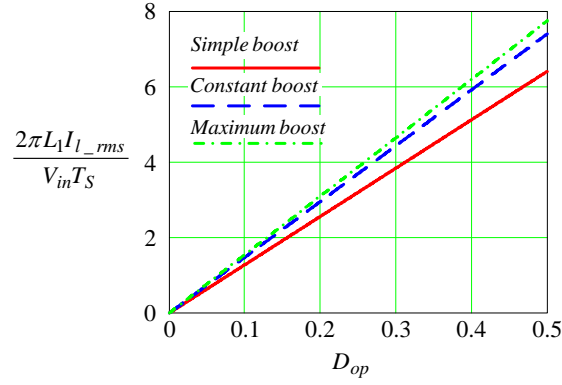


Fig. 36. Normalized Z-source inductor inductance of CF-ZSI with three control methods.

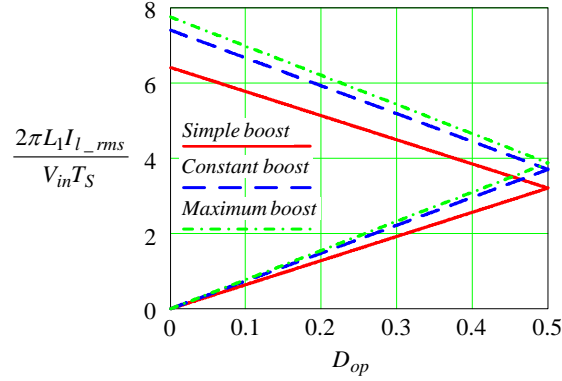


Fig. 37. Normalized Z-source inductor inductance comparison of CF-ZSI and CF-qZSI with three control methods.

3. Input Inductor

a. Inductor Current Stress

Because we already know

$$I_{in_peak} = \frac{2\sqrt{2}}{\sqrt{3}} \frac{1}{BM} I_{l_rms} \quad (146)$$

So the input inductor current of CF-ZSI is the same as the CF-qZSI.

Simple boost:

$$I_{in_peak} = \frac{2\sqrt{2}I_{l_rms}}{\sqrt{3}} \frac{1-2D_{op}}{1-D_{op}} \quad (147)$$

Constant boost:

$$I_{in_peak} = \sqrt{2}I_{l_rms} \frac{1-2D_{op}}{1-D_{op}} \quad (148)$$

Maximum boost:

$$I_{in_peak} = \frac{3\sqrt{2}I_{l_rms}}{\pi} \frac{1-2D_{op}}{1-D_{op}} \quad (149)$$

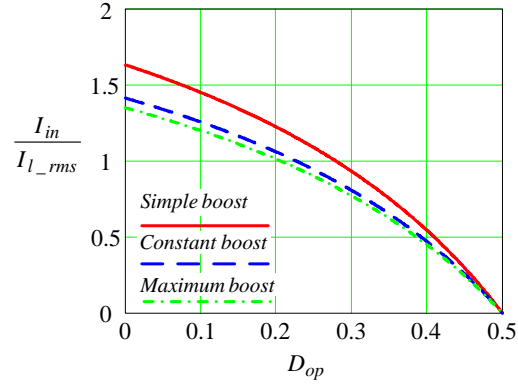


Fig. 38 Normalized input inductor current stresses with three control methods.

b. Inductance

If open zero state existed the inductance is

$$L_{in} = \frac{V_{in}D_{op}T_S}{30\%I_{in}} \quad (150)$$

$$L_{in} = D_{op}BM \frac{\sqrt{3}V_{in}T_S}{30\%2\sqrt{2}I_{l_rms}} \quad (151)$$

So the CF-qZSI input inductor inductance requirement is the same with CF-ZSI.

Plug in all the BM of three control methods.

$$L_{in} = D_{op} \frac{1-D_{op}}{1-2D_{op}} \frac{\sqrt{3}V_{in}T_S}{30\%2\sqrt{2}I_{l_rms}} \quad (152)$$



(153)

$$L_{in} = D_{op} \frac{1 - D_{op}}{1 - 2D_{op}} \frac{\pi V_{in} T_S}{30\% 3\sqrt{2} I_{l_rms}} \quad (154)$$

Assume the base is:

$$\frac{V_{in} T_S}{2\pi I_{l_rms}} \quad (155)$$

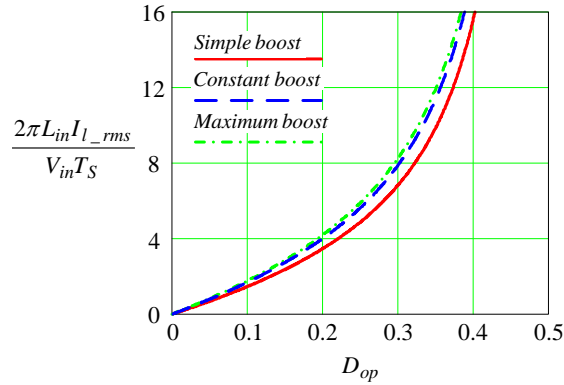


Fig. 39. Normalized inductance of input inductor with three control methods.

c. Current-fed Trans-quasi-Z-source Inverter (CF-trans-qZSI)

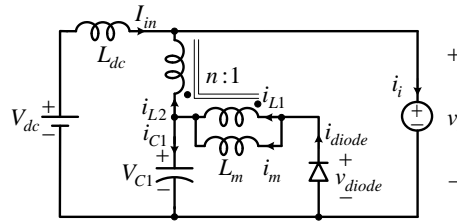


Fig. 40 CF-trans-qZSI

1. Z-source Capacitor

a. Capacitor Voltage Stress

The capacitor is DC capacitor, the inductor voltage under steady state is zero, so the capacitor voltage is V_{in} . Because the minimum input voltage can be reduced to output the same peak voltage, the capacitor voltage stress can be also reduced.

b. Capacitor Current Stress

The Z-source capacitor current is near zero during the non-open zero state operation.

The capacitor C1 current is $I_{L1} + I_{in} + I_m$ during the open zero state, and the capacitor current is $-I_{L2}$ during other states, because the inductor L2 current is positive, $-I_{L2}$ is a negative value.

And the capacitor RMS current is

$$I_{C_rms} = \sqrt{D_{op}(I_{L1} + I_{in} + I_m)^2 + (1 - D_{op})(-I_{L2})^2} \quad (156)$$

Because according to the capacitor current balance



$$I_{L1} + I_{in} + I_m = I_{L2} \quad (157)$$

Because the transformer current has the relationship:

$$\frac{I_{L2}}{I_{L1}} = \frac{1}{n} \quad (158)$$

During the (1-Dop) state, the $I_{L1} = I_m = nI_{L2}$

During the Dop state, $I_{L1} = nI_{L2} = nI_{in}$, so the above capacitor balance equation can be derived to

$$-\frac{1}{n}(1 - D_{op})I_m + (I_{in} + nI_{in} + I_m)D_{op} = 0 \quad (159)$$

So we can derive that:

$$I_m = \frac{n(n+1)D_{op}}{1 - (n+1)D_{op}} I_{in} \quad (160)$$

Because the inductor L1 only conducts during the diode conduction time, so the current of L1 is $nI_{L2} = nI_{in}$, So

$$I_{L1} + I_{in} + I_m = nI_{in} + I_{in} + \frac{n(n+1)D_{op}}{1 - (n+1)D_{op}} I_{in} = \frac{(n+1)(1 - D_{op})}{1 - (1+n)D_{op}} I_{in} \quad (161)$$

When the non open zero states happens, the inductor L2 current is 1/n of the magnetizing current, as follows

$$I_{L2} = \frac{(n+1)D_{op}}{1 - (n+1)D_{op}} I_{in} \quad (162)$$

and the inductor L2 current is $-I_{in}$ during the open zero state. So by plug in all the inductor current using input current: we can get

$$I_{C_rms} = \sqrt{D_{op}\left(\frac{(n+1)(1 - D_{op})}{1 - (1+n)D_{op}} I_{in}\right)^2 + (1 - D_{op})\left(-\frac{(n+1)D_{op}}{1 - (n+1)D_{op}} I_{in}\right)^2} \quad (163)$$

$$I_{C_rms} = \frac{I_{in}(n+1)}{1-(n+1)D_{op}} \sqrt{D_{op}(1-D_{op})} \quad (164)$$

From this equation, we can derive that, for the trans-Z-source inverter, the capacitor requirement is not reduced at all, even when $n=1$, the capacitor current rms value is still 2 times bigger than the traditional Z-source.

Because the output rated line current is constant during the change of duty cycle, so we should choose the output line current as the base to determine the required rms current of the capacitor. The capacitor rms current can be indicated by rated line current as follows

$$I_{C_rms} = \frac{(n+1)}{1-(n+1)D_{op}} \sqrt{D_{op}(1-D_{op})} \frac{2\sqrt{2}}{\sqrt{3}} \frac{I_{l_rms}}{BM} \quad (165)$$

So we can plug in the BM of three different control methods.

Simple boost

$$BM_{simple} = \frac{1-D_{op}}{1-(n+1)D_{op}} \quad (166)$$

Constant boost:

$$BM_{constant} = \frac{2}{\sqrt{3}} \frac{1-D_{op}}{1-(n+1)D_{op}} \quad (167)$$

Maximum boost:

$$BM_{maximum} = \frac{2\pi}{3\sqrt{3}} \frac{1-D_{op}}{1-(n+1)D_{op}} \quad (168)$$

So

$$I_{C_rms_simple} = (n+1) \sqrt{\frac{D_{op}}{1-D_{op}}} \frac{2\sqrt{2}}{\sqrt{3}} I_{l_rms} \quad (169)$$

$$I_{C_rms_constant} = (n+1) \sqrt{\frac{D_{op}}{1-D_{op}}} \sqrt{2} I_{l_rms} \quad (170)$$

$$I_{C_rms_maximum} = (n+1) \sqrt{\frac{D_{op}}{1-D_{op}}} \frac{3\sqrt{2}}{\pi} I_{l_rms} \quad (171)$$

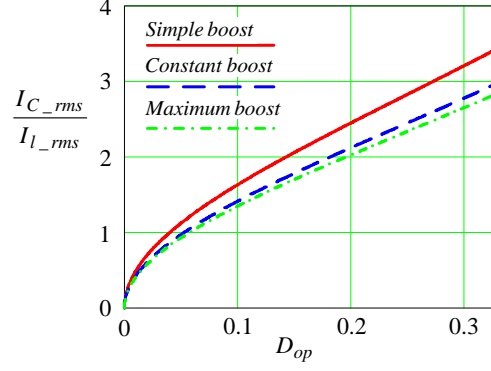


Fig. 41. The normalized capacitor current stresses with three control methods when $n=2$.

c. Capacitance

$$C = \frac{I_C D_{op} T_S}{\Delta V} = \frac{(n+1)(1-D_{op})}{1-(1+n)D_{op}} \frac{2\sqrt{2}}{\sqrt{3}} \frac{I_{L_rms}}{BM} \frac{D_{op} T_S}{10\% V_{in}} \quad (172)$$

Plug in the BM of three different control method.

$$C_{simple} = (n+1) \frac{2\sqrt{2}}{\sqrt{3}} I_{L_rms} \frac{D_{op} T_S}{10\% V_{in}} \quad (173)$$

$$C_{constant} = (n+1) \sqrt{2} I_{L_rms} \frac{D_{op} T_S}{10\% V_{in}} \quad (174)$$

$$C_{maximum} = (n+1) \frac{3\sqrt{2}}{\pi} I_{L_rms} \frac{D_{op} T_S}{10\% V_{in}} \quad (175)$$

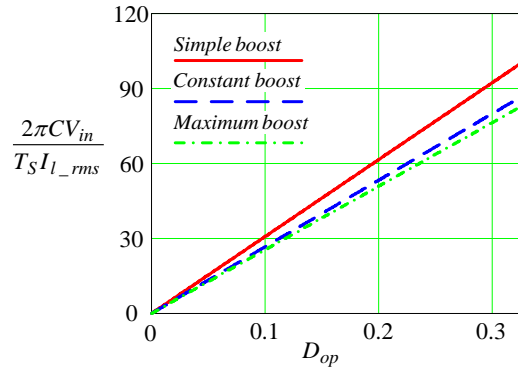


Fig. 42. Capacitance requirement comparison with three control methods

2. Z-source Inductor

a. Inductor Current Stress

Because the inductor L1 current during the open zero state is

$$I_{L_1} = I_{L1} + I_m \quad (176)$$

$$I_{L_1} = nI_{in} + \frac{n(n+1)D_{op}}{1-(n+1)D_{op}} I_{in} = \frac{n}{1-(n+1)D_{op}} I_{in} \quad (177)$$

Because the inductor current is not continuous, we need the RMS current to estimate the power loss.

$$I_{L_1_rms} = \sqrt{\left(\frac{n}{1-(n+1)D_{op}} I_{in} \right)^2 D_{op}} = \frac{n}{1-(n+1)D_{op}} I_{in} \sqrt{D_{op}} \quad (178)$$

$$I_{L_1_rms} = \frac{n}{1-(n+1)D_{op}} \sqrt{D_{op}} \frac{2\sqrt{2}}{\sqrt{3}} \frac{I_{l_rms}}{BM} \quad (179)$$

Plug in BM of three control methods.

$$I_{L_1_rms_simple} = n \frac{\sqrt{D_{op}}}{1-D_{op}} \frac{2\sqrt{2}}{\sqrt{3}} I_{l_rms} \quad (180)$$

$$I_{L_1_rms_constant} = n \frac{\sqrt{D_{op}}}{1-D_{op}} \sqrt{2} I_{l_rms} \quad (181)$$

$$I_{L_1_rms_maximum} = n \frac{\sqrt{D_{op}}}{1-D_{op}} \frac{3\sqrt{2}}{\pi} I_{l_rms} \quad (182)$$

The inductor L2 current during the open zero state is

$$I_{L_2} = I_{in} \quad (183)$$

The inductor L2 current during the non open zero state is

$$I_{L_2} = \frac{1}{n} I_m = \frac{(n+1)D_{op}}{1-(n+1)D_{op}} I_{in} \quad (184)$$

So the inductor L2 current rms value is

$$I_{L_2_rms} = \sqrt{I_{in}^2 D_{op} + \left(\frac{(n+1)D_{op}}{1-(n+1)D_{op}} I_{in} \right)^2 (1-D_{op})} \quad (185)$$

$$I_{L_2_rms} = \frac{I_{in}}{1-(n+1)D_{op}} \sqrt{D_{op} \left[1 - 2(n+1)D_{op} + (n+1)^2 D_{op} \right]} \quad (186)$$

$$I_{L_2_rms} = \frac{1}{1-(n+1)D_{op}} \frac{2\sqrt{2}}{\sqrt{3}} \frac{I_{l_rms}}{BM} \sqrt{D_{op} \left[1 - 2(n+1)D_{op} + (n+1)^2 D_{op} \right]} \quad (187)$$

Plug in three control methods:

$$I_{L_2_rms_simple} = \frac{2\sqrt{2}}{\sqrt{3}} \frac{I_{l_rms}}{1-D_{op}} \sqrt{D_{op} \left[1 - 2(n+1)D_{op} + (n+1)^2 D_{op} \right]} \quad (188)$$

$$I_{L_2_rms_constant} = \sqrt{2} \frac{I_{l_rms}}{1-D_{op}} \sqrt{D_{op} \left[1 - 2(n+1)D_{op} + (n+1)^2 D_{op} \right]} \quad (189)$$

$$I_{L_2_rms_maximum} = \frac{3\sqrt{2}}{\pi} \frac{I_{l_rms}}{1-D_{op}} \sqrt{D_{op} \left[1 - 2(n+1)D_{op} + (n+1)^2 D_{op} \right]} \quad (190)$$

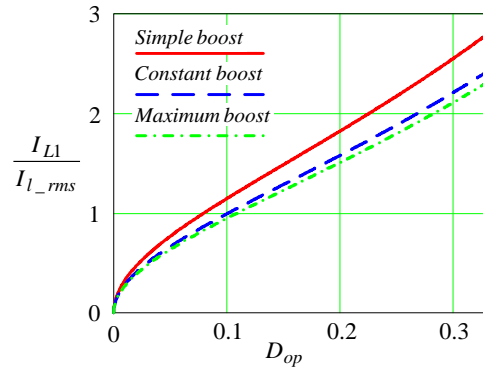


Fig. 43. Normalized Inductor L1 current stress of three control methods when n=2.

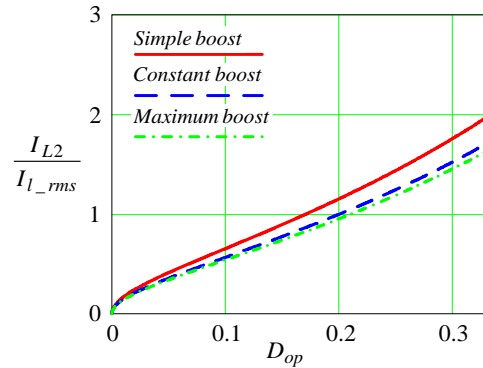


Fig. 44. Normalized Inductor L2 current stress of three control methods when n=2.

b. Inductance

Z-source Inductance L1.

$$L_1 = \frac{V_{in} D_{op} T_S}{\Delta I} = \frac{V_{in} D_{op} T_S}{30\% I_m} \quad (191)$$

We can get the inductance requirement of three different control methods.

Simple boost:

$$L_1 = \frac{V_{in} D_{op} T_S}{\Delta I} = \frac{\sqrt{3}}{2\sqrt{2}} \frac{V_{in} D_{op} T_S (1 - D_{op})}{30\% n I_{l_rms}} \quad (192)$$

Constant boost:

$$L_1 = \frac{V_{in} D_{op} T_S}{\Delta I} = \frac{1}{\sqrt{2}} \frac{V_{in} D_{op} T_S (1 - D_{op})}{30\% n I_{l_rms}} \quad (193)$$

Maximum boost:

$$L_1 = \frac{V_{in} D_{op} T_S}{\Delta I} = \frac{\pi}{3\sqrt{2}} \frac{V_{in} D_{op} T_S (1 - D_{op})}{30\% n I_{l_rms}} \quad (194)$$

Make $\frac{V_{in} T_S}{I_{l_rms} 2\pi}$ be the base, we can get the normalized inductance value. We noticed that we need to time 2π to the equation.

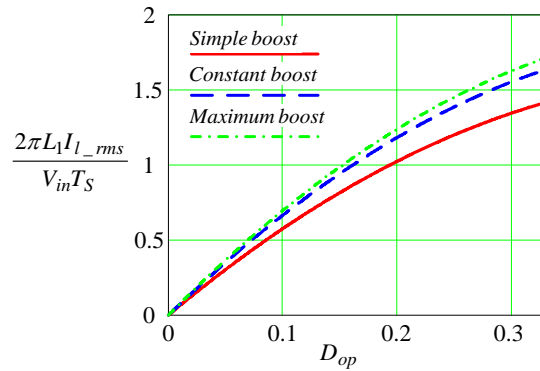


Fig. 45. Normalized L1 inductance of CF-qZSI when n=2

Z-source inductance L2

$$L_2 = n^2 L_1 \quad (195)$$

The L2 is determined by the turns ratio.

3. Input Inductor

a. Inductor Current Stress

Because we already know

$$I_{in_peak} = \frac{2\sqrt{2}}{\sqrt{3}} \frac{1}{BM} I_{l_rms} \quad (196)$$

Plug in the BM of three control methods:

Simple boost:

$$I_{in_peak} = \frac{2\sqrt{2}}{\sqrt{3}} \frac{1-(n+1)D_{op}}{1-D_{op}} I_{l_rms} \quad (197)$$

Constant boost:

$$I_{in_peak} = \sqrt{2} \frac{1-(n+1)D_{op}}{1-D_{op}} I_{l_rms} \quad (198)$$

Maximum boost:

$$I_{in_peak} = \frac{3\sqrt{2}}{\pi} \frac{1-(n+1)D_{op}}{1-D_{op}} I_{l_rms} \quad (199)$$

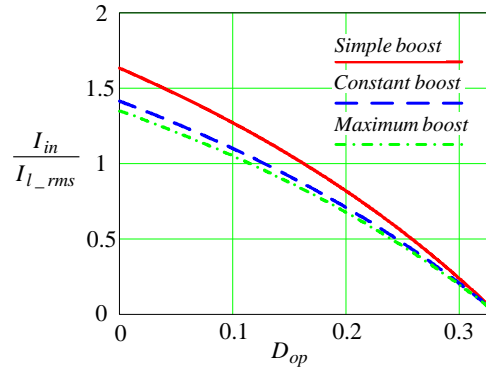


Fig. 46. Normalized input Inductor current stress of three control methods when n=2.

b. Inductance

$$L_{in} = \frac{nV_{in}D_{op}T_S}{\Delta I} = \frac{nV_{in}D_{op}T_S}{30\%I_{in}} \quad (200)$$

Plug in BM of three control method and replace I_{in} with I_{l_rms} we can get

Simple boost:

$$L_{in} = \frac{nV_{in}D_{op}T_S}{\Delta I} = \frac{\sqrt{3}}{2\sqrt{2}} \frac{nV_{in}D_{op}T_S(1-D_{op})}{30\%(1-(n+1)D_{op})I_{l_rms}} \quad (201)$$

Constant boost:

$$L_{in} = \frac{nV_{in}D_{op}T_S}{\Delta I} = \frac{1}{\sqrt{2}} \frac{nV_{in}D_{op}T_S(1-D_{op})}{30\%(1-(n+1)D_{op})I_{l_rms}} \quad (202)$$

Maximum boost:

$$L_{in} = \frac{nV_{in}D_{op}T_S}{\Delta I} = \frac{\pi}{3\sqrt{2}} \frac{nV_{in}D_{op}T_S(1-D_{op})}{30\%(1-(n+1)D_{op})I_{l_rms}} \quad (203)$$

Also make $\frac{V_{in}T_S}{I_{l_rms}2\pi}$ as the base, we can get the normalized input inductance requirement.

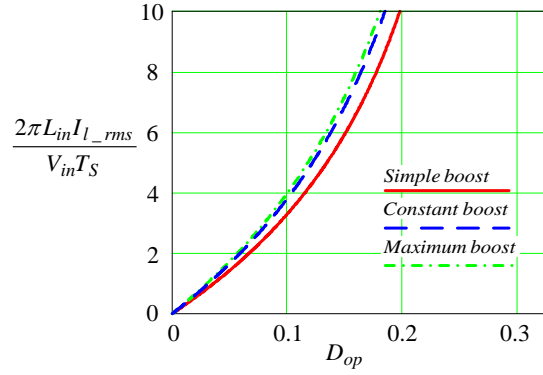


Fig. 47. Normalized inductance of input inductor with three control methods when n=2.

d. Current-fed Trans-Z-source Inverter (CF-trans-ZSI)

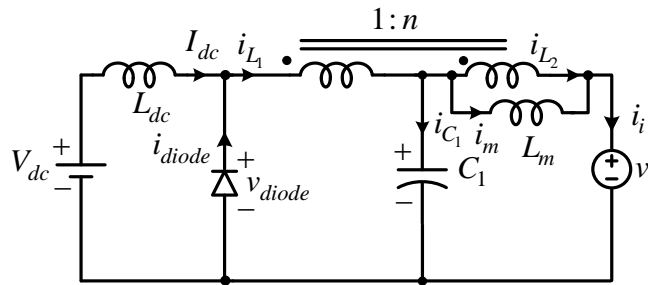


Fig. 48. CF-trans-ZSI

1. Z-source Capacitor

a. Capacitor Voltage Stress

The capacitor is in dc side, the inductor voltage under steady state is zero, so the capacitor voltage is V_{in} . Because the minimum input voltage can be reduced, the capacitor voltage stress can be also reduced. The trans-ZSI is the same with trans-qZSI at this point.

b. Capacitor Current Stress

The capacitor C1 current is always $I_{L1} - I_{L2}$. During the open zero state, the inductor L2 current is zero, and all the current used to flow through inductor L2 times turns ratio flow through the diode. So the L1 current during this open zero state is $I_{L1} = I_{in} + nI_{L2}$ and the capacitor current is $I_C = I_{in} + nI_{L2}$, during other states, the capacitor current are $I_C = I_{in} - I_{L2}$ which are negative value.

And the capacitor RMS current is

$$I_{C_rms} = \sqrt{D_{op}(I_{in} + nI_{L2})^2 + (1 - D_{op})(I_{in} - I_{L2})^2} \quad (204)$$

Because according to the capacitor current balance

$$D_{op}(I_{in} + nI_{L2}) + (1 - D_{op})(I_{in} - I_{L2}) = 0 \quad (205)$$

So the relationship of I_{in} and I_{L2} can be derived as follows.

$$I_{L2} = \frac{1}{1 - (n+1)D_{op}} I_{in} \quad (206)$$

and the inductor L2 current is 0 during the open zero state.

So by plugging in all the inductor current using input current: we can get

$$I_{C_rms} = \sqrt{D_{op}\left(I_{in} + n\frac{1}{1 - (n+1)D_{op}}I_{in}\right)^2 + (1 - D_{op})\left(I_{in} - \frac{1}{1 - (n+1)D_{op}}I_{in}\right)^2} \quad (207)$$

$$I_{C_rms} = \frac{I_{in}(n+1)}{1 - (n+1)D_{op}} \sqrt{D_{op}(1 - D_{op})} \quad (208)$$

The trans-ZSI has the same form of trans-qZSI of capacitor rms current. From this equation, we can also derive that, for the trans-Z-source inverter, the capacitor requirement is not reduced at all, even when $n=1$, the capacitor current rms value is still 2 times bigger than the traditional Z-source. Because the output rated line current is constant during the change of duty cycle, so we should choose the output line current as the base to determine the required rms current of the capacitor.

So the capacitor rms current can be indicated by rated line current as follows

$$I_{C_rms} = \frac{(n+1)}{1 - (n+1)D_{op}} \sqrt{D_{op}(1 - D_{op})} \frac{2\sqrt{2}}{\sqrt{3}} \frac{I_{l_rms}}{BM} \quad (209)$$

So we can plug in the BM of three different control method.

For simple boost

$$BM_{simple} = \frac{1-D_{op}}{1-(n+1)D_{op}} \quad (210)$$

For constant boost:

$$BM_{constant} = \frac{2}{\sqrt{3}} \frac{1-D_{op}}{1-(n+1)D_{op}} \quad (211)$$

For maximum boost:

$$BM_{maximum} = \frac{2\pi}{3\sqrt{3}} \frac{1-D_{op}}{1-(n+1)D_{op}} \quad (212)$$

So

$$I_{C_rms_simple} = (n+1) \sqrt{\frac{D_{op}}{1-D_{op}}} \frac{2\sqrt{2}}{\sqrt{3}} I_{l_rms} \quad (213)$$

$$I_{C_rms_constant} = (n+1) \sqrt{\frac{D_{op}}{1-D_{op}}} \sqrt{2} I_{l_rms} \quad (214)$$

$$I_{C_rms_maximum} = (n+1) \sqrt{\frac{D_{op}}{1-D_{op}}} \frac{3\sqrt{2}}{\pi} I_{l_rms} \quad (215)$$

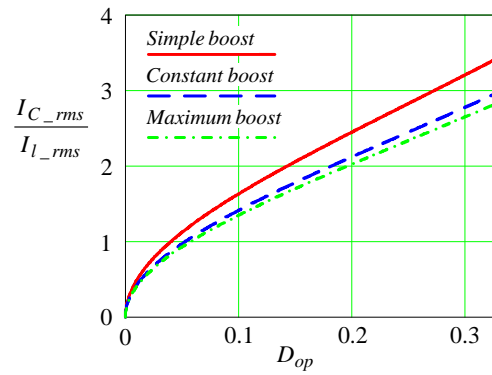


Fig. 49. The normalized capacitor current stresses with three control methods when n=2.

c. Capacitance

$$C = \frac{I_C D_{op} T_S}{\Delta V} = \frac{(n+1)(1-D_{op})}{1-(1+n)D_{op}} \frac{2\sqrt{2}}{\sqrt{3}} \frac{I_{l_rms}}{BM} \frac{D_{op} T_S}{10\% V_{in}} \quad (216)$$

Plug in the BM of three different control method.

$$C_{simple} = (n+1) \frac{2\sqrt{2}}{\sqrt{3}} I_{l_rms} \frac{D_{op} T_S}{10\% V_{in}} \quad (217)$$

$$C_{constant} = (n+1) \sqrt{2} I_{l_rms} \frac{D_{op} T_S}{10\% V_{in}} \quad (218)$$

$$C_{maximum} = (n+1) \frac{3\sqrt{2}}{\pi} I_{l_rms} \frac{D_{op} T_S}{10\% V_{in}} \quad (219)$$

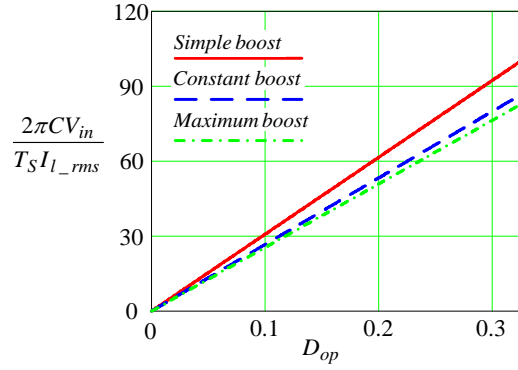


Fig. 50. Capacitance requirement comparison with three control methods.

2. Z-source Inductor

a. Inductor Current Stress

Because the inductor L1 current during the open zero state is

$$I_{L1} = I_{in} + nI_{L2} \quad (220)$$

$$I_{L1} = I_{in} + \frac{n}{1-(n+1)D_{op}} I_{in} = \frac{(n+1)(1-D_{op})}{1-(n+1)D_{op}} I_{in} \quad (221)$$

And the inductor L1 current during the non open zero state is

$$I_{L1} = I_{in} \quad (222)$$

Because the inductor current is not continuous, we need the RMS current to estimate the power loss.

$$I_{L1_rms} = \sqrt{\left(\frac{(n+1)(1-D_{op})}{1-(n+1)D_{op}} I_{in}\right)^2 D_{op} + I_{in}^2 (1-D_{op})} = \frac{I_{in} \sqrt{(1-D_{op})[1+(n^2-1)D_{op}]}}{1-(n+1)D_{op}} \quad (223)$$

$$I_{L_1_rms} = \frac{\sqrt{(1-D_{op})[1+(n^2-1)D_{op}]}}{1-(n+1)D_{op}} \frac{2\sqrt{2}}{\sqrt{3}} \frac{I_{l_rms}}{BM} \quad (224)$$

With three control method.

$$I_{L1_rms_simple} = \frac{\sqrt{(1-D_{op})[1+(n^2-1)D_{op}]}}{1-D_{op}} \frac{2\sqrt{2}}{\sqrt{3}} I_{l_rms} \quad (225)$$

$$I_{L1_rms_constant} = \frac{\sqrt{(1-D_{op})[1+(n^2-1)D_{op}]}}{1-D_{op}} \sqrt{2} I_{l_rms} \quad (226)$$

$$I_{L1_rms_maximum} = \frac{\sqrt{(1-D_{op})[1+(n^2-1)D_{op}]}}{1-D_{op}} \frac{3\sqrt{2}}{\pi} I_{l_rms} \quad (227)$$

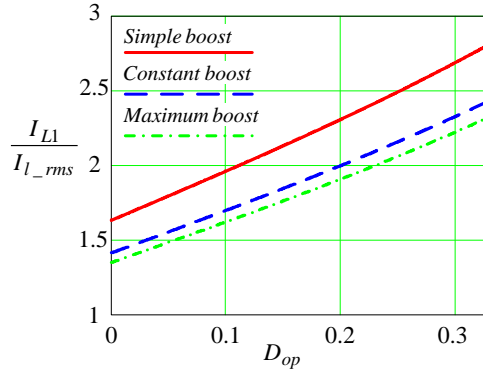


Fig. 51. Normalized Inductor L1 current stress of three control methods when n=2.

The inductor L2 current during the open zero state is zero

The inductor L2 current during the non open zero state is

$$I_{L2} = \frac{1}{1-(n+1)D_{op}} I_{in} \quad (228)$$

So the inductor L2 current rms value is

$$I_{L2_rms} = \frac{1}{1-(n+1)D_{op}} I_{in} \sqrt{(1-D_{op})} \quad (229)$$

$$I_{L2_rms} = \frac{1}{1-(n+1)D_{op}} \frac{2\sqrt{2}}{\sqrt{3}} \frac{I_{l_rms}}{BM} \sqrt{1-D_{op}} \quad (230)$$

Plug in three control method:

$$I_{L2_rms_simple} = \frac{2\sqrt{2}}{\sqrt{3}} \frac{I_{l_rms}}{1-D_{op}} \sqrt{1-D_{op}} \quad (231)$$

$$I_{L2_rms_constant} = \sqrt{2} \frac{I_{l_rms}}{1-D_{op}} \sqrt{1-D_{op}} \quad (232)$$

$$I_{L2_rms_maximum} = \frac{3\sqrt{2}}{\pi} \frac{I_{l_rms}}{1-D_{op}} \sqrt{1-D_{op}} \quad (233)$$

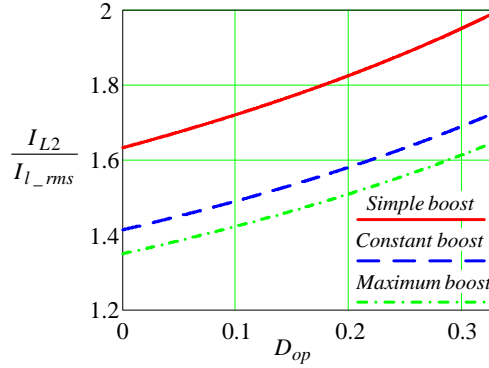


Fig. 52. Normalized Inductor L2 current stress of three control methods when n=2.

b. Inductance

Z-source Inductance L2. (or the magnetic inductance)

Actually, because the Z-source inductor current is not continuous, so, what we need to do is design the magnetic inductor properly.

Although during the open zero state the current i_i , through the inductor L2 and L_m together is zero. But actually, that is the combination of the current through magnetic inductance and the transformer secondary side. The current through L_m is not zero.

$$L_m = \frac{nV_{in}D_{op}T_S}{\Delta I} = \frac{nV_{in}D_{op}T_S}{30\%I_m} \quad (234)$$

Because $I_m = I_{L2}$ We can get the inductance requirement of three different control method.

Simple boost:

$$L_m = L_2 = \frac{nV_{in}D_{op}T_S}{\Delta I} = \frac{\sqrt{3}}{2\sqrt{2}} \frac{nV_{in}D_{op}T_S(1-D_{op})}{30\%I_{l_rms}} \quad (235)$$

Constant boost:

$$L_m = L_2 = \frac{nV_{in}D_{op}T_S}{\Delta I} = \frac{1}{\sqrt{2}} \frac{nV_{in}D_{op}T_S(1-D_{op})}{30\%I_{l_rms}} \quad (236)$$

Maximum boost:

$$L_m = L_2 = \frac{nV_{in}D_{op}T_S}{\Delta I} = \frac{\pi}{3\sqrt{2}} \frac{nV_{in}D_{op}T_S(1-D_{op})}{30\%I_{l_rms}} \quad (237)$$

Make $\frac{V_{in}T_S}{I_{l_rms}2\pi}$ be the base, we can get the normalized inductance value. We noticed that we need to time 2π to the equation.

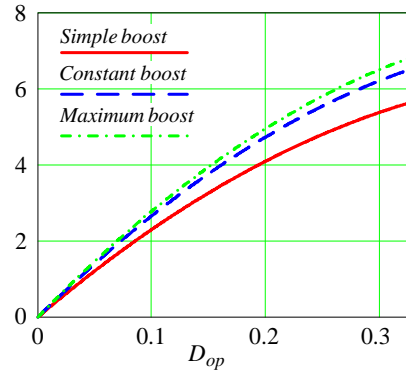


Fig. 53. Normalized L2 inductance of CF-ZSI when $n=2$

Z-source inductance L_1

$$L_2 = n^2 L_1 \quad (238)$$

The L_1 is determined by the turns ratio.

3. Input Inductor

a. Inductor Current Stress

Because we already know

$$I_{in_peak} = \frac{2\sqrt{2}}{\sqrt{3}} \frac{1}{BM} I_{l_rms} \quad (239)$$

Simple boost:

$$I_{in_peak} = \frac{2\sqrt{2}}{\sqrt{3}} \frac{1-(n+1)D_{op}}{1-D_{op}} I_{l_rms} \quad (240)$$

Constant boost:

$$I_{in_peak} = \sqrt{2} \frac{1-(n+1)D_{op}}{1-D_{op}} I_{l_rms} \quad (241)$$

Maximum boost:

$$I_{in_peak} = \frac{3\sqrt{2}}{\pi} \frac{1-(n+1)D_{op}}{1-D_{op}} I_{l_rms} \quad (242)$$

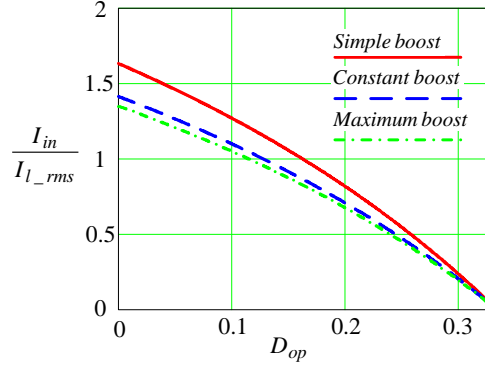


Fig. 54. Normalized input Inductor current stress of three control methods when n=2.

b. Inductance

$$L_{in} = \frac{V_{in} D_{op} T_S}{\Delta I} = \frac{n V_{in} D_{op} T_S}{30\% I_{in}} \quad (243)$$

Plug in (376), (377), (378) we can get

Simple boost:

$$L_{in} = \frac{n V_{in} D_{op} T_S}{\Delta I} = \frac{\sqrt{3}}{2\sqrt{2}} \frac{V_{in} D_{op} T_S (1-D_{op})}{30\% (1-(n+1)D_{op}) I_{l_rms}} \quad (244)$$

Constant boost

$$L_{in} = \frac{V_{in} D_{op} T_S}{\Delta I} = \frac{1}{\sqrt{2}} \frac{V_{in} D_{op} T_S (1-D_{op})}{30\% (1-(n+1)D_{op}) I_{l_rms}} \quad (245)$$

Maximum boost:

$$L_{in} = \frac{V_{in} D_{op} T_S}{\Delta I} = \frac{\pi}{3\sqrt{2}} \frac{V_{in} D_{op} T_S (1-D_{op})}{30\% (1-(n+1)D_{op}) I_{l_rms}} \quad (246)$$

Also make $\frac{V_{in} T_S}{I_{l_rms} 2\pi}$ as the base, we can get the normalized input inductance requirement.

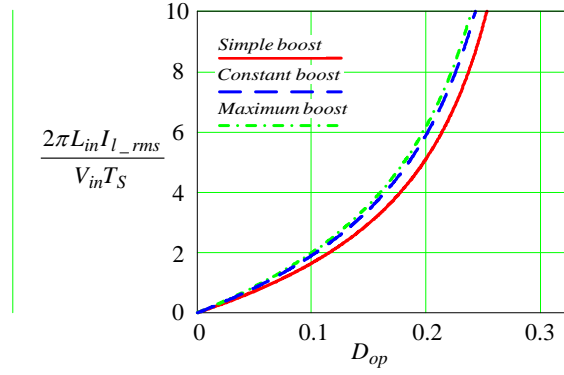


Fig. 55. Normalized inductance of input inductor with three control methods when $n=2$.

IV. 55 kW Current-fed Inverter Design

1. Design Specifications:

- Power Rating: 55 kW
- Input Battery Voltage: 260 V
- Output line-to-line Voltage: 0~500 V
- Switching frequency: 10 kHz
- Transformer turns ratio: 2
- Power Density: 4.9 kg/kW, 15.5 L/kW
- Efficiency: 93.8~94%

2. Design Procedures:

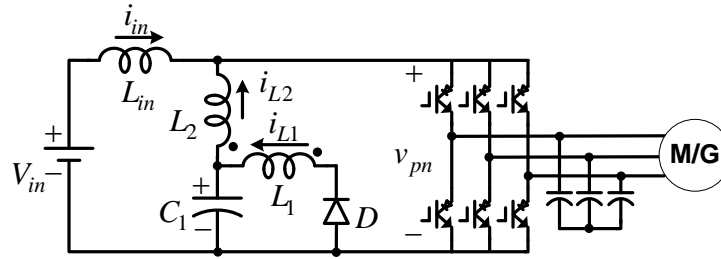


Fig. 56. Current-fed trans-qZSI circuit

Fig. 56 shows the Current-fed trans-quasi Z-source inverter we use for designing the 55 kW inverter.

The motor operate at constant torque region in the buck mode, and the motor operate at constant power region in the boost mode.

The mode change operation point should be already the maximum power output at the constant torque and constant power transition.

a. **Switching Device:**

1. Voltage Stress:

In no-open zero state cases, which means the equivalent dc voltage is larger than V_{in} , the device peak voltage stress is the peak output line-to-line voltage. If the device is not conducting in one phase leg, the other device in the same phase leg is conducting. One of the devices of other phase leg is also conducting, so the line-to-line voltage will add to the device.

$$V_S = \sqrt{2}V_{ll} \quad (247)$$

In the cases when the equivalent dc voltage is smaller than V_{in} , we have to run the system with open zero state. The positive device voltage stress will be

$$+V_S = V_{CN} + V_{phase} = \frac{1}{2}V_{PN} + V_{phase} = \frac{3}{2}V_{in} + V_{phase} = \frac{3}{2}V_{in} + \frac{\sqrt{2}}{\sqrt{3}}V_{ll} \quad (248)$$

The edge condition happens when the third harmonic injection is used with the modulation index equals to 1.15. The output peak line-to-line voltage is 300 V. Assuming the output peak line-to-line voltage is x axis, the 300 V peak line-to-line voltage is

$$\frac{\frac{300}{\frac{260*3}{\sqrt{2}}}}{\sqrt{2}} = \frac{300}{780} \approx 0.385 \quad (249)$$

How the device voltage stress is determined is explained as follows. During the open zero state, all the devices are off. The device voltage stress is $V_S = V_{CN} + V_{phase}$, the V_{CN} is the capacitor center voltage.

In average, the device voltage in a 60 Hz period should be $\frac{1}{2}V_{PN} = \frac{3}{2}V_{in}$, because the phase voltage in a 60 Hz period should be zero. So the capacitor neutral voltage during the open zero state should be $V_{CN} = \frac{1}{3}(V_A + V_B + V_C) = \frac{1}{3} \frac{3}{2}V_{PN} = \frac{1}{2}V_{PN} = \frac{3}{2}V_{in}$.

The negative device voltage stress is still the peak line-to-line voltage, which is

$$-V_S = \sqrt{2}V_{ll} \quad (250)$$

Fig. 57 shows the device voltage stress according to the change of the output voltage.

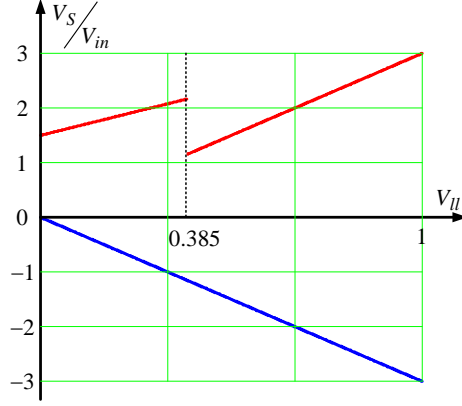


Fig. 57 Device voltage stress.

So, the device peak voltage stress should be $V_S = \pm 3V_{in} = \pm 780V$, we need to choose the 1200 V reverse blocking device.

2. Current Stress

a. Boost mode

For the circuit operating at boost mode, the peak switch current is the peak input current.

The peak input current equals to the peak average input current plus 30% peak to peak input current ripple.

$$I_{in_peak} = I_{in_ave} + 15\% I_{in_ave} = \frac{P_o}{V_{in}} (1 + 0.15) \quad (251)$$

So, the peak switch current is

$$I_{S_peak} = I_{in_peak} = \frac{P_o}{V_{in}} (1 + 0.15) = 243 \text{ A} \quad (252)$$

The average switch current is one third of the peak input average current.

$$I_{S_ave} = \frac{1}{3} I_{in_ave} = \frac{1}{3} \frac{P_o}{V_{in}} = \frac{1}{3} \frac{55000}{260} \approx 70 \text{ A} \quad (253)$$

So, the switching device with current rating equals to 200 A could be chosen for the boost mode operation.

b. Buck mode

In buck mode, we can first calculate the I_{pn} , because $I_{S_pk} = I_{pn_pk}$ and the $I_{S_ave} = \frac{1}{3} I_{pn_ave}$.
Because

$$I_{pn} = I_{in} + I_{L2} \quad (254)$$

And

$$I_{L2} = \frac{(1+n)D_{op}}{1-(1+n)D_{op}} I_{in} \quad (255)$$

We can derive that

$$I_{pn_pk} = \frac{I_{in}}{1-(n+1)D_{op}} \quad (256)$$

Because

$$I_{pn_ave} = (1-D_{op})I_{pn_pk} \quad (257)$$

We can derive that

$$I_{pn_ave} = \frac{1-D_{op}}{1-(n+1)D_{op}} I_{in} \quad (258)$$

Because, according to the power balance equation, we know that

$$I_{in} = \frac{2\sqrt{2}I_{l_rms}}{\sqrt{3}BM} \quad (259)$$

So we can derive from (258) and (259).

$$I_{pn_ave} = \frac{1-D_{op}}{1-(n+1)D_{op}} \frac{2\sqrt{2}}{\sqrt{3}BM} I_{l_rms} \quad (260)$$

Because from simple boost we have

$$BM_{simple} = \frac{1-D_{op}}{1-(n+1)D_{op}} \quad (261)$$

For constant boost we have

$$BM_{constant} = \frac{2}{\sqrt{3}} \frac{1-D_{op}}{1-(n+1)D_{op}} \quad (262)$$

For maximum boost we have

$$BM_{maximum} = \frac{2\pi}{3\sqrt{3}} \frac{1-D_{op}}{1-(n+1)D_{op}} \quad (263)$$

By plug in this BM values into (260), we can get

$$I_{pn_ave_simple} = \frac{2\sqrt{2}}{\sqrt{3}} I_{l_rms} \quad (264)$$

$$I_{pn_ave_constant} = \sqrt{2} I_{l_rms} \quad (265)$$

$$I_{pn_ave_maximum} = \frac{3\sqrt{2}}{\pi} I_{l_rms} \quad (266)$$

Because the switch current stress is one third of the I_{pn} , for the switch current stress in three different control method we can get

$$I_{S_ave_simple} = \frac{2\sqrt{2}}{3\sqrt{3}} I_{l_rms} \quad (267)$$

$$I_{S_ave_constant} = \frac{\sqrt{2}}{3} I_{l_rms} \quad (268)$$

$$I_{S_ave_maximum} = \frac{\sqrt{2}}{\pi} I_{l_rms} \quad (269)$$

Fig. 58 shows the normalized switch average current stress with the change of the line voltage. We can derive that, by using the constant boost control, the current stress of the device in buck mode is the same with the current stress in boost mode. We can choose also choose the device with the current rating 200 A for our design.

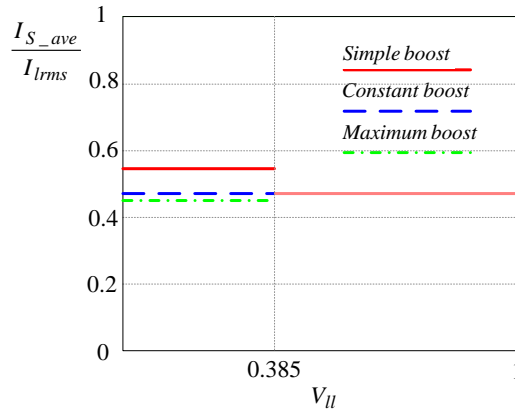


Fig. 58 Normalized switch average current stress to load current with the change of line voltage.

3. Device chosen

The 1200 V and 200 A reverse blocking (RB) IGBT could be chosen for the design. But the RB-IGBT with the rating 1200 V 200 A is not existed, we can estimate the conduction loss, switching loss based on the 1200 V 100 A RB-IGBT from Fuji. Fig. 59 shows the characteristics of the RB-IGBT from

Fuji. The saturation voltage of a 200 A device can be considered as the same with the 100 A device. And the switching loss of a 200 A device can be considered as twice bigger than the 100 A device.

Voltage	Current	$V_{CE(sat)}$ @125°C	E_{on} @125°C	E_{off} @125°C	E_{rr} @125°C	Conditions
600V	100A	2.8V	6mJ	4mJ	1mJ	$E_{dc}=300V, I_c=100A,$ $V_{GE}=\pm 15V, R_g=33\Omega$
	200A	2.8V	12mJ	8mJ	2mJ	$E_{dc}=300V, I_c=200A,$ $V_{GE}=\pm 15V, R_g=16\Omega$
1200V	50A	2.8V	10mJ	5mJ	4mJ	$E_{dc}=600V, I_c=50A,$ $V_{GE}=\pm 15V, R_g=33\Omega$
	100A	2.8V	20mJ	10mJ	8mJ	$E_{dc}=600V, I_c=100A,$ $V_{GE}=\pm 15V, R_g=16\Omega$

Fig. 59. Characteristics of RB-IGBT from Fuji.

4. Conduction loss

Because the $V_{ce(sat)}=2.8V$, the average switch current is 70 A. So the six switches conduction loss are

$$P_{S_con} = 6V_{CE(sat)}I_{S_ave} = 6 * 2.8 * 70 = 1176 \text{ W} \quad (270)$$

5. Switching loss

The switching loss should include the E_{on} and E_{off} . according to Fig. 59, the switching loss of the 100 A device is twice bigger than the 50 A device, so we can assume the switching loss of 200 A device twice bigger than the 100 A device. Because the inverter reach the peak power at the transition knee point of the constant torque and the constant power region, the inverter switching loss can be estimated at this point. Because the inverter voltage stress is 300 V at this point, the switching loss testing voltage is 600 V. The switching loss data in the datasheet should also be reduced by twice to estimate.

$$E_{on_200A} = 40mJ \quad (271)$$

$$E_{off_200A} = 20mJ \quad (272)$$

$$E_{sw_200A} = E_{on_200A} + E_{off_200A} = 60mJ \quad (273)$$

So, the total six switches switching loss under 10 kHz switching frequency are

$$E_{sw_total} = 6 \left(\frac{1}{2} E_{sw_200A} \right) f_S = 6 * 30m * 10k = 1800 \text{ W} \quad (274)$$

Actually, in the line frequency cycle, the voltage stress across the device will change, the real switching loss of the device when the inverter is working will be much smaller than the estimated value here.

6. Size and weight

Because the 1200 V 100 A device from Fuji provide has 18 switches inside. So, 6 switches with doubled current rating can be still sealed in the similar package. So we can use the 1200 V 100 A RB-IGBT from Fuji to estimate the device size and weight.

The size of the device is

$$Vol_S = 14cm * 11cm * 2cm = 308cm^3 = 0.308L \quad (275)$$

The weight of the device is about

$$W_S = 850g \quad (276)$$

b. Diode:

1. Voltage Stress:

a. Boost mode

If we don't have open zero states during the operation, the diode voltage stress is

$$V_D = (1 + \frac{1}{n})V_{in} = \frac{3}{2}V_{in} = 390V \quad (277)$$

b. Buck mode

If we have open zero states during the operation, the diode voltage stress is

$$V_D = (1 + \frac{1}{2})V_{in} = 390V \quad (278)$$

So a 600 V diode could be chosen.

2. Current Stress:

a. Boost mode

In boost mode without open zero states, the diode will not conducting, so the current stress is zero

b. Buck mode

In buck mode with open zero states. The diode will conduct. The peak diode current is

$$I_{D_pk} = \frac{n}{1-(n+1)D_{op}} \frac{P_o}{V_i} = \frac{n}{1-(n+1)D_{op}} I_{in} \quad (279)$$

Because I_{in} is not constant during the whole period. So we should use the output current as the base. Because we have

$$3V_{p_rms} I_{l_rms} \cos \varphi = P_{o_peak} = V_{in} I_{in_peak} \quad (280)$$

And

$$V_{p_rms} = \frac{2\sqrt{2}}{3\sqrt{3}} \frac{1}{BM \cos \delta} V_{in} \quad (281)$$

We can derive the relationship of I_{in} and I_{l_rms} . So

$$I_{in} = \frac{2\sqrt{2}}{\sqrt{3}BM} I_{l_rms} \quad (282)$$

So we plug in (282) into (279), and we can get.

$$I_{D_pk} = \frac{n}{1-(n+1)D_{op}} I_{in} = \frac{n}{1-(n+1)D_{op}} \frac{2\sqrt{2}}{\sqrt{3}BM} I_{l_rms} \quad (283)$$

For simple boost we have

$$BM_{simple} = \frac{1-D_{op}}{1-(n+1)D_{op}} \quad (284)$$

So

$$I_{D_pk_simple} = \frac{n}{1-(n+1)D_{op}} I_{in} = n \frac{2\sqrt{2}}{\sqrt{3}(1-D_{op})} I_{l_rms} = \frac{4\sqrt{2}I_{l_rms}}{\sqrt{3}(1-D_{op})} \quad (285)$$

For constant boost we have

$$BM_{constant} = \frac{2}{\sqrt{3}} \frac{1-D_{op}}{1-(n+1)D_{op}} \quad (286)$$

So

$$I_{D_pk_constant} = \frac{n}{1-(n+1)D_{op}} I_{in} = n \frac{\sqrt{2}}{1-D_{op}} I_{l_rms} = \frac{2\sqrt{2}}{1-D_{op}} I_{l_rms} \quad (287)$$

For Maximum boost we have

$$BM_{maximum} = \frac{2\pi}{3\sqrt{3}} \frac{1-D_{op}}{1-(n+1)D_{op}} \quad (288)$$

So

$$I_{D_pk_maximum} = \frac{n}{1-(n+1)D_{op}} I_{in} = \frac{3n}{\pi} \frac{\sqrt{2}}{1-D_{op}} I_{l_rms} \quad (289)$$

So the average current through diode are

$$I_{D_ave_simple} = \frac{4\sqrt{2}D_{op}I_{l_rms}}{\sqrt{3}(1-D_{op})} \quad (290)$$

$$I_{D_ave_constant} = \frac{2\sqrt{2}D_{op}}{1-D_{op}} I_{l_rms} \quad (291)$$

$$I_{D_ave_maximum} = \frac{3n}{\pi} \frac{\sqrt{2}D_{op}}{1-D_{op}} I_{l_rms} \quad (292)$$

Fig. 60 and Fig. 61 show the normalized diode current peak current and average current respectively.

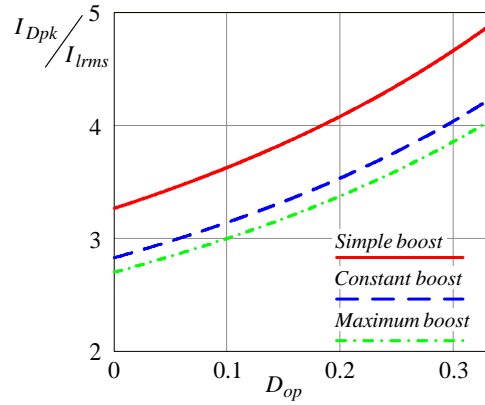


Fig. 60. Normalized diode peak current stress to output line current.

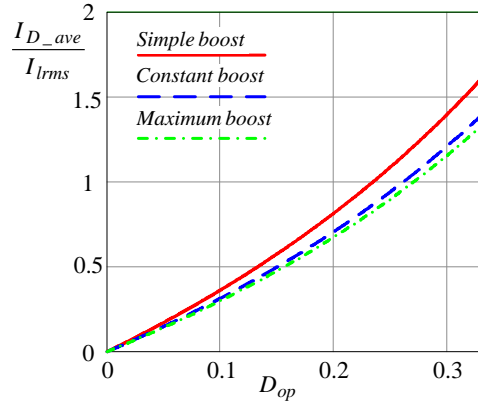


Fig. 61. Normalized diode average current stress to output line current

Because the rated line current is about 149.2 A, if we use constant boost control. At the $D_{op}=0.33$.

$$I_{Dpk} = \frac{2\sqrt{2}}{1-d} = \frac{2\sqrt{2}}{1-\frac{1}{3}} = 4.2, \text{ the peak current is } 626 \text{ A.}$$

Also assume the constant boost control is used, the peak average current of diode is 211 A

3. Device chosen

So, a 600 V 600 A diode could be chosen for the design. The 600V 800A diode QRS0680T30 from powerex is chosen as the diode.

Electrical Characteristics, $T_J=25^\circ\text{C}$ unless otherwise specified

Characteristics	Symbol	Test Conditions	Min.	Typ.	Max	Units
Peak Reverse Leakage Current	I_{RRM}	Rated V_{RRM}	-	-	2	mA
Peak On-State Voltage	V_{FM}	$I_F=800\text{A}$	-	2.0	2.8	Volts
		$I_F=600\text{A}$	-	1.7	-	
Reverse Recovery Time	t_{rr}	$I_F = 800\text{A}$, $di/dt = -1600\text{A}/\mu\text{s}$	-	-	110	ns
Reverse Recovery Charge	Q_{rr}	$I_F=800\text{A}$, $di/dt = -1600\text{A}/\mu\text{s}$	-	2.16	-	μC

Fig. 62. Electrical characteristics of QRS06080T30 from powerex.

4. Conduction loss

Because the forward voltage drop is 1.7 V and the peak average current is 211 A, So the diode conduction loss is

$$P_{diode} = V_{fwd} I_{D_ave} = 358.7 \text{ W} \quad (293)$$

And the reverse recovery loss of the diode is

$$E_{Drr} = QV_D f_S = 2.16\mu * 600 * 10k = 12.96 \text{ W} \quad (294)$$

5. Size and weight

The diode size is

$$Vol_D = 94mm * 34mm * 30mm = 0.09588L = 5.85in^3 \quad (295)$$

The diode weight is

$$W_D = 220g \quad (296)$$

c. Z-source Capacitor**1. Voltage Stress**

The Z-source capacitor voltage stress is the input voltage plus the capacitor voltage ripple. So, for a 260 V input voltage, the 300 V capacitor should work.

2. Current Stress**a. Boost mode**

During the boost mode, the capacitor current ripple is depended on the secondary inductor current ripple. And the inductor current ripple depends on the inductance and the voltage across the inductor and the duty cycle. During this mode, the Z-source inductor is not transferring or storing energy, so the idle current of the Z-source inductor is quite small, the current stress of the Z-source capacitor should be determined by the buck mode conditions.

b. Buck mode

The capacitor C1 current is $I_{L1} + I_{in} + I_m$ during the open zero state, and the capacitor current is $-I_{L2}$ during other states, because the inductor L2 current is positive, $-I_{L2}$ is a negative value.

And the capacitor RMS current is

$$I_{C_rms} = \sqrt{D_{op}(I_{L1} + I_{in} + I_m)^2 + (1 - D_{op})(-I_{L2})^2} \quad (297)$$

According to the capacitor current balance

$$(-I_{L2})(1 - D_{op}) + (I_{in} + I_{L1} + I_m)D_{op} = 0 \quad (298)$$

The transformer current has the relationship.

$$\frac{I_{L2}}{I_{L1}} = \frac{1}{n} \quad (299)$$

During the (1-Dop) state, the $I_{L1} = I_m = nI_{L2}$

During the Dop state, $I_{L1} = nI_{L2} = nI_{in}$, so the above capacitor balance equation can be derived to

$$-\frac{1}{n}(1 - D_{op})I_m + (I_{in} + nI_{in} + I_m)D_{op} = 0 \quad (300)$$

We can derive that:

$$I_m = \frac{n(n+1)D_{op}}{1 - (n+1)D_{op}} I_{in} \quad (301)$$

Because the inductor L1 only conducts during the diode conduction time, so the current of L1 is $nI_{L2} = nI_{in}$, So

$$I_{L1} + I_{in} + I_m = nI_{in} + I_{in} + \frac{n(n+1)D_{op}}{1 - (n+1)D_{op}} I_{in} = \frac{(n+1)(1 - D_{op})}{1 - (1+n)D_{op}} I_{in} \quad (302)$$

When the non open zero states happens, the inductor L2 current is 1/n of the magnetizing current, as follows

$$I_{L2} = \frac{(n+1)D_{op}}{1 - (n+1)D_{op}} I_{in} \quad (303)$$

and the inductor L2 current is $-I_{in}$ during the open zero state.

So by plug in all the inductor current using input current: we can get

$$I_{C_rms} = \sqrt{D_{op} \left(\frac{(n+1)(1-D_{op})}{1-(1+n)D_{op}} I_{in} \right)^2 + (1-D_{op}) \left(-\frac{(n+1)D_{op}}{1-(n+1)D_{op}} I_{in} \right)^2} \quad (304)$$

$$I_{C_rms} = \frac{I_{in}(n+1)}{1-(n+1)D_{op}} \sqrt{D_{op}(1-D_{op})} \quad (305)$$

From this equation, we can derive than that, for the trans-Z-source inverter, the capacitor requirement is not reduced at all, even when n=1, the capacitor current rms value is still 2 times bigger than the traditional Z-source.

Because the output rated line current is constant during the change of duty cycle, so we should choose the output line current as the base to determine the required rms current of the capacitor. Because,

$$3V_{p_rms}I_{l_rms} \cos \varphi = P_{o_peak} = V_{in}I_{in_peak} \quad (306)$$

And

$$V_{p_rms} = \frac{2\sqrt{2}}{3\sqrt{3}} \frac{1}{BM \cos \varphi} V_{in} \quad (307)$$

According to the above two equations,

$$I_{in_peak} = \frac{2\sqrt{2}}{\sqrt{3}} \frac{I_{l_rms}}{BM} \quad (308)$$

The capacitor rms current can be indicated by rated line current as follows

$$I_{C_rms} = \frac{(n+1)}{1-(n+1)D_{op}} \sqrt{D_{op}(1-D_{op})} \frac{2\sqrt{2}}{\sqrt{3}} \frac{I_{l_rms}}{BM} \quad (309)$$

We can plug in the BM of three different control methods.

For simple boost

$$BM_{simple} = \frac{1-D_{op}}{1-(n+1)D_{op}} \quad (310)$$

For constant boost:

$$BM_{constant} = \frac{2}{\sqrt{3}} \frac{1-D_{op}}{1-(n+1)D_{op}} \quad (311)$$

For maximum boost:

$$BM_{maximum} = \frac{2\pi}{3\sqrt{3}} \frac{1-D_{op}}{1-(n+1)D_{op}} \quad (312)$$

So

$$I_{C_rms_simple} = (n+1) \sqrt{\frac{D_{op}}{1-D_{op}}} \frac{2\sqrt{2}}{\sqrt{3}} I_{l_rms} \quad (313)$$

$$I_{C_rms_constant} = (n+1) \sqrt{\frac{D_{op}}{1-D_{op}}} \sqrt{2} I_{l_rms} \quad (314)$$

$$I_{C_rms_maximum} = (n+1) \sqrt{\frac{D_{op}}{1-D_{op}}} \frac{3\sqrt{2}}{\pi} I_{l_rms} \quad (315)$$

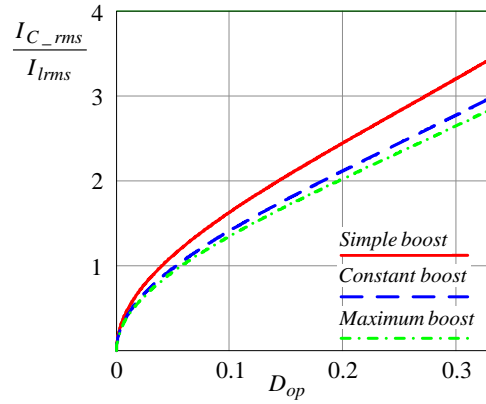


Fig. 63 Normalized capacitor RMS current stress with n=2

If constant control is utilized, the maximum capacitor ripple current stress is about 3 times output line current. So a capacitor with 450 A RMS current is required.

3. Capacitance

a. Boost mode

During the boost mode, the current flow into the capacitor is the current flow through the inductor L2, only triangle current flow through, the capacitance requirement is relatively smaller than the buck mode. And the capacitance should also be determined by the buck mode operation.

b. Buck mode

Capacitance:

$$C = \frac{I_C D_{op} T_S}{\Delta V} = \frac{(n+1)(1-D_{op})}{1-(1+n)D_{op}} \frac{2\sqrt{2}}{\sqrt{3}} \frac{I_{l_rms}}{BM} \frac{D_{op} T_S}{10\% V_{in}} \quad (316)$$

Plug in the BM of three different control method.

$$C_{simple} = (n+1) \frac{2\sqrt{2}}{\sqrt{3}} I_{l_rms} \frac{D_{op} T_S}{10\% V_{in}} \quad (317)$$

$$C_{constant} = (n+1) \sqrt{2} I_{l_rms} \frac{D_{op} T_S}{10\% V_{in}} \quad (318)$$

$$C_{maximum} = (n+1) \frac{3\sqrt{2}}{\pi} I_{l_rms} \frac{D_{op} T_S}{10\% V_{in}} \quad (319)$$

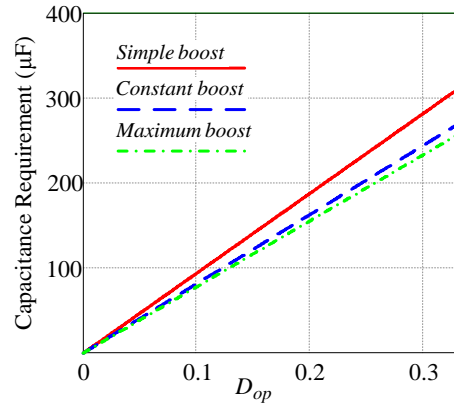


Fig. 64. Capacitance requirement.

4. Device chosen

So the Z-source capacitor only needs a 300 Vdc with about 450 Arms.

In order to meet the current stress requirement, 4 of UL34Q157K in parallel are chosen to meet the current stress requirement.

5. Power loss

Because the RMS of the chosen capacitor is 0.47mOhm, 4 of them in parallel ESR=0.12mOhm.

So the peak power loss is

$$P_{ZC_peak} = I_{rms_peak}^2 ESR_{ZC} = 450^2 * 0.12m = 24.3 \text{ W} \quad (320)$$

6. Size and weight

The size of the chosen capacitor is

$$Vol_{ZC} = 4 * \pi \left(\frac{0.833}{2} \right)^2 * 0.4 = 0.87L \quad (321)$$

The weight of the capacitor is

$$W_{ZC} = 300g * 4 = 1200g \quad (322)$$

d. Z-source Inductor

1. Current Stress

a. Boost mode

For the Z-source inductor L1 in boost mode, the current stress is zero. For the Z-source inductor L2 in boost mode, the current stress is the capacitor current stress, which is also about zero.

b. Buck mode

Because the inductor L1 current during the open zero state is

$$I_{L_1} = I_{L1} + I_m \quad (323)$$

$$I_{L_1} = nI_{in} + \frac{n(n+1)D_{op}}{1-(n+1)D_{op}} I_{in} = \frac{n}{1-(n+1)D_{op}} I_{in} \quad (324)$$

Because the inductor current is not continuous, we need the RMS current to estimate the power loss.

$$I_{L_1_rms} = \sqrt{\left(\frac{n}{1-(n+1)D_{op}} I_{in} \right)^2 D_{op}} = \frac{n}{1-(n+1)D_{op}} I_{in} \sqrt{D_{op}} \quad (325)$$

$$I_{L_1_rms} = \frac{n}{1-(n+1)D_{op}} \sqrt{D_{op}} \frac{2\sqrt{2}}{\sqrt{3}} \frac{I_{l_rms}}{BM} \quad (326)$$

With three control methods,

$$I_{L_1_rms_simple} = n \frac{\sqrt{D_{op}}}{1-D_{op}} \frac{2\sqrt{2}}{\sqrt{3}} I_{l_rms} \quad (327)$$

$$I_{L_1_rms_constant} = n \frac{\sqrt{D_{op}}}{1-D_{op}} \sqrt{2} I_{l_rms} \quad (328)$$

$$I_{L_1_rms_maximum} = n \frac{\sqrt{D_{op}}}{1-D_{op}} \frac{3\sqrt{2}}{\pi} I_{l_rms} \quad (329)$$

The inductor L2 current during the open zero state is

$$I_{L_2} = I_{in} \quad (330)$$

The inductor L2 current during the non open zero state is

$$I_{L_2} = \frac{1}{n} I_m = \frac{(n+1)D_{op}}{1-(n+1)D_{op}} I_{in} \quad (331)$$

So the inductor L2 current rms value is

$$I_{L_2_rms} = \sqrt{I_{in}^2 D_{op} + \left(\frac{(n+1)D_{op}}{1-(n+1)D_{op}} I_{in} \right)^2 (1-D_{op})} \quad (332)$$

$$I_{L_2_rms} = \frac{I_{in}}{1-(n+1)D_{op}} \sqrt{D_{op} \left[1-2(n+1)D_{op} + (n+1)^2 D_{op} \right]} \quad (333)$$

$$I_{L_2_rms} = \frac{1}{1-(n+1)D_{op}} \frac{2\sqrt{2}}{\sqrt{3}} \frac{I_{l_rms}}{BM} \sqrt{D_{op} \left[1-2(n+1)D_{op} + (n+1)^2 D_{op} \right]} \quad (334)$$

Plug in three control methods:

$$I_{L_2_rms_simple} = \frac{2\sqrt{2}}{\sqrt{3}} \frac{I_{l_rms}}{1-D_{op}} \sqrt{D_{op} \left[1-2(n+1)D_{op} + (n+1)^2 D_{op} \right]} \quad (335)$$

$$I_{L_2_rms_constant} = \sqrt{2} \frac{I_{l_rms}}{1-D_{op}} \sqrt{D_{op} \left[1-2(n+1)D_{op} + (n+1)^2 D_{op} \right]} \quad (336)$$

$$I_{L_2_rms_maximum} = \frac{3\sqrt{2}}{\pi} \frac{I_{l_rms}}{1-D_{op}} \sqrt{D_{op} \left[1-2(n+1)D_{op} + (n+1)^2 D_{op} \right]} \quad (337)$$

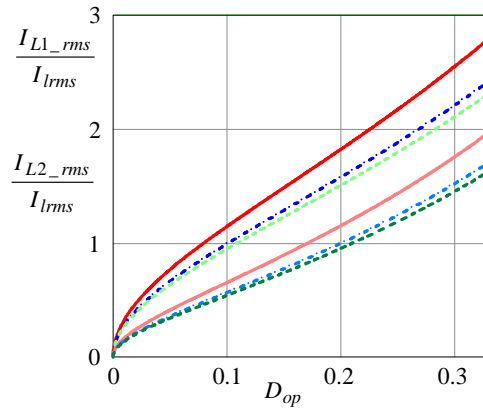


Fig. 65 Z-source Inductor current stress (top three line is I_{L1} , bottom three line is I_{L2} with three control method).

So the peak current stress of inductor L1 and L2 happens when the $D_{op}=0.33$, because the peak line current is about 150 A, So, the peak current stress of L1 and L2 are

$$I_{L1_pk_rms} = 2 \frac{\sqrt{\frac{1}{3}}}{1 - \frac{1}{3}} \sqrt{2} * 150 = 367.35 A \quad (338)$$

$$I_{L2_pk_rms} = \sqrt{2} \frac{150}{1 - \frac{1}{3}} \sqrt{\frac{1}{3} \left[1 - 2(2+1)\frac{1}{3} + (2+1)^2 \frac{1}{3} \right]} = 259.8 A \quad (339)$$

2. Inductance

a. Boost mode

The Z-source inductor will not work during the boost mode.

b. Buck mode

Z-source Inductance L1.

$$L_1 = \frac{V_{in} D_{op} T_S}{\Delta I} = \frac{V_{in} D_{op} T_S}{30\% I_m} \quad (340)$$

According to (324) and (376), (377), (378). We can get the inductance requirement of three different control method.

Simple boost:

$$L_{1m} = \frac{V_{in} D_{op} T_S}{\Delta I} = \frac{\sqrt{3}}{2\sqrt{2}} \frac{V_{in} T_S (1 - D_{op})}{30\% n(n+1) I_{l_rms}} \quad (341)$$

Constant boost:

$$L_{1m} = \frac{V_{in} D_{op} T_S}{\Delta I} = \frac{1}{\sqrt{2}} \frac{V_{in} T_S (1 - D_{op})}{30\% n(n+1) I_{l_rms}} \quad (342)$$

Maximum boost:

$$L_{1m} = \frac{V_{in} D_{op} T_S}{\Delta I} = \frac{\pi}{3\sqrt{2}} \frac{V_{in} T_S (1 - D_{op})}{30\% n(n+1) I_{l_rms}} \quad (343)$$

Make $\frac{V_{in} T_S}{I_{l_rms} 2\pi}$ be the base, we can get the normalized inductance value. We noticed that we need to time 2π to the equation.

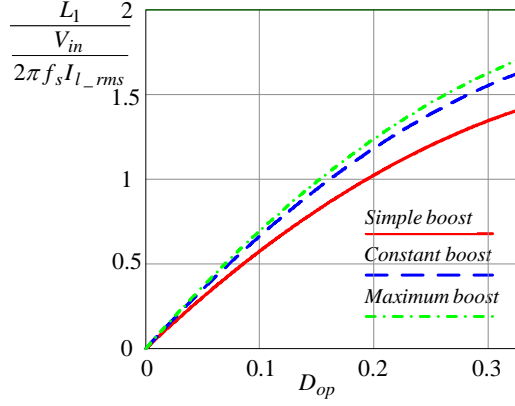


Fig. 66 Normalized Z-source inductance L1 requirement.

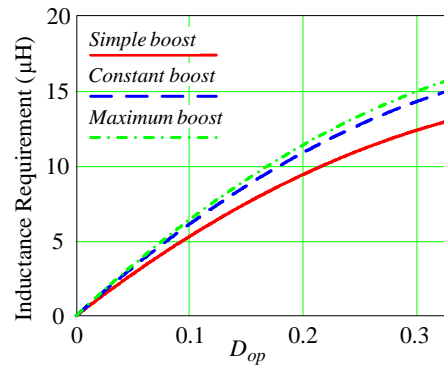


Fig. 67. Z-source inductor L1 inductance requirement.

Z-source inductance L2

$$L_2 = n^2 L_1 \quad (344)$$

The L2 is determined by the turns ratio.

3. Core chosen and inductor design

a. Select Core

We decide to choose the core using AP method

$$AP = A_w \cdot A_e = \frac{I_{rms}}{J_{Cu} K_0} \frac{L \cdot I_{peak}}{\Delta B} \quad (345)$$

A_w is the window area

A_e is the cross section area

J_{Cu} is the current density

K_0 is the use of the window coefficient

So

$$AP = A_w \cdot A_e = \frac{I_{rms}}{J_{Cu} K_0} \frac{L \cdot I_{peak}}{\Delta B} = \frac{367 \cdot 10^4}{500 \cdot 0.6} \frac{15 \mu \cdot 636}{0.3} = 389 \text{ cm}^4 \quad (346)$$

In order to meet the requirement of AP, we choose the amorphous alloy AMCC500 as our core, The AP of the AMCC500 is as follows,

$$AP_{AMCC500} = 383.4 \text{ cm}^4 \quad (347)$$

b. Number of turns

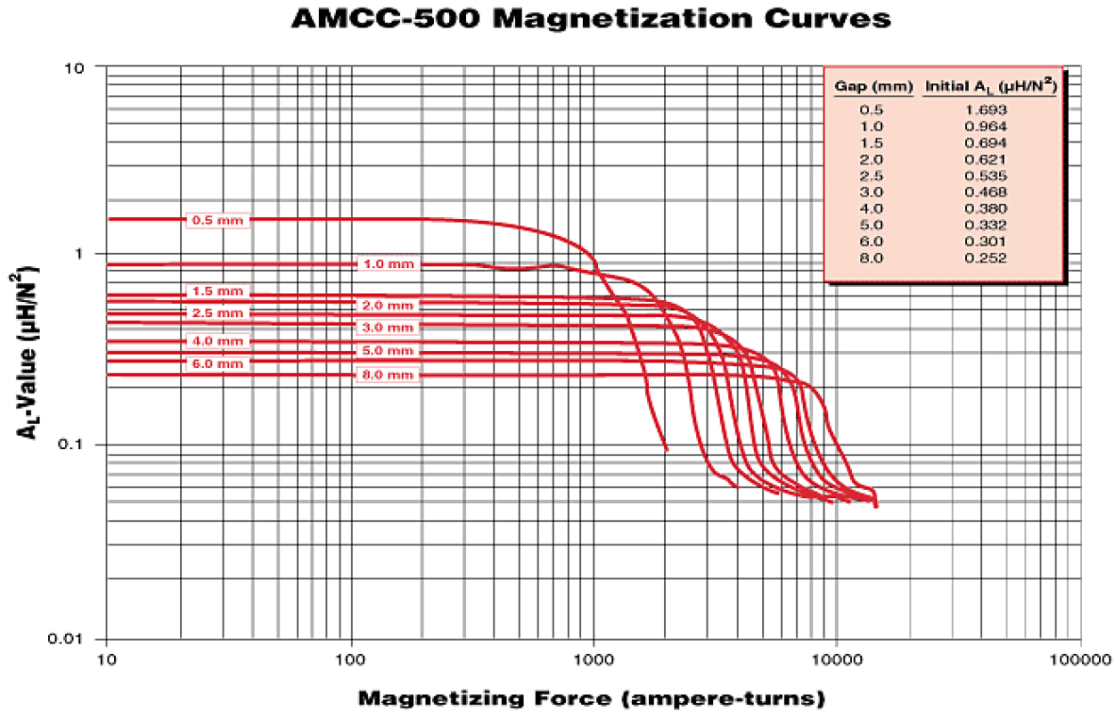


Fig. 68. Inductance value of AMCC-500 core.

We should choose the correct air gap by iteration and 3 mm air gap is finally chosen.

$$A_L \approx 400 \text{ nH} / N^2 \quad (348)$$

So the number of turns is

$$N_T = \sqrt{\frac{L_1}{A_L}} = \sqrt{\frac{15 \mu\text{H}}{0.4 \mu\text{H} / N^2}} = 6.1 \approx 6 \text{ turns} \quad (349)$$

The total MMF is

$$\text{MMF} = N_T I_{peak} = 6 \cdot 636 = 3816 \text{ A-turns} \quad (350)$$

The new A_L after the inductance drop is

$$A_{L_new} \approx 350 \text{ nH} / N^2 \quad (351)$$

So the final inductance value will be

$$L_{1_new} = N_T^2 A_{L_new} = 12.6 \text{ } \mu\text{H} \quad (352)$$

c. Core size and loss

The total weight of our core is

$$W_{Core} = 2.89 \text{ kg} \quad (353)$$

Because the core loss of AMCC500 is

$$P_L = 6.5 B^{1.74} F^{1.51} \quad (354)$$

Fig. 69 shows the core loss curve of this core. B is Tesla, and f is kHz. $P_L = \text{W/kg}$. From the figure, we can derive that, when our $B=0.3 \text{ T}$, $P_{L_30\text{kHz}} = 136 \text{ W/kg}$. So the total core loss is

$$P_{core_30\text{kHz}} = P_{L_30\text{kHz}} \cdot W_{core} = 136 \text{ W/kg} \cdot 2.89 \text{ kg} = 393 \text{ W} \quad (355)$$

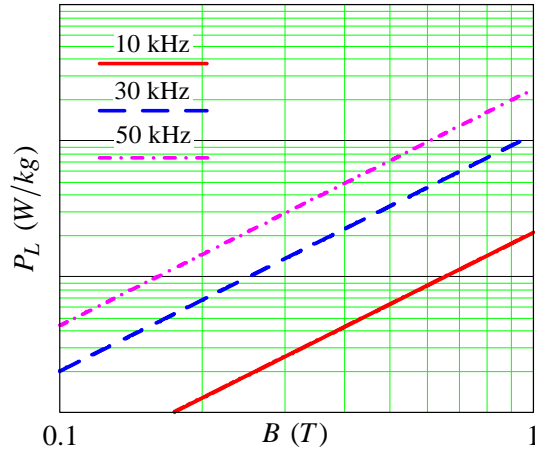


Fig. 69. AMCC500 core loss curve

4. Winding chosen and copper loss

a. Choose the correct winding size

Because the inductor L1 current stress is

$$I_{L1_rms_peak} = 367 \text{ A} \quad (356)$$

The copper foil is selected as the winding. Assume the current density is

$$J_{Cu} = 5 \text{ A/mm}^2 \quad (357)$$

The section area of the copper foil should be

$$A_{L1} = \frac{I_{L1_rms_peak}}{J_{Cu}} = \frac{367}{5} = 73.4 \text{ mm}^2 \quad (358)$$

We need to consider the skin effect and calculate the thickness of the copper foil.

Because in 100C $\rho_{Cu} = 2.3 \cdot 10^{-8} \Omega \cdot \text{m}$, and because $\mu_{Cu} = 4\pi \cdot 10^{-7}$, So we can calculate the skin depth of the copper in 10 kHz is

$$\delta_{30K} = \sqrt{\frac{\rho_{Cu}}{\pi \mu_{Cu} f_S}} = \sqrt{\frac{2.3 \cdot 10^{-8}}{\pi \cdot 1.257 \cdot 10^{-6} \cdot 30 \cdot 10^3}} = 0.44 \text{ mm} \quad (359)$$

The 0.02" thickness of the copper foil should be chosen. The width of the copper should be chosen according to the core size which is 80 mm

The section area of the chosen copper foil is

$$A_{L1} = 80 \cdot 0.508 = 40.64 \text{ mm}^2 \quad (360)$$

Two layers of primary side should be used.

The current density is

$$J_{Cu_1} = \frac{I_{L1_rms_peak}}{2A_{L1}} = 4.59 \text{ A/mm}^2 \quad (361)$$

The secondary winding should be 12 turns.

So the inductor L2 current stress is

$$I_{L2_rms_peak} = 260 \text{ A} \quad (362)$$

So the section area of the copper foil should be

$$A_{L2} = \frac{I_{L2_rms_peak}}{J_{Cu}} = \frac{260}{5} = 52 \text{ mm}^2 \quad (363)$$

The same copper foil as the primary side can be also chosen. The current density of the secondary winding is

$$J_{Cu_2} = \frac{I_{L2_rms_peak}}{A_{L2}} = \frac{260}{40.64} = 6.4 A/mm^2 \quad (364)$$

b. Copper Loss

The primary winding is 6 turns with 2 layers and the secondary winding is 12 turns with 1 layer. The length of one turn copper foil could be

$$l_{turn} = 4 * 2 + 7 * 2 = 22cm \quad (365)$$

So the total length of the primary winding is $l_{pri_winding} = l_{turn} * 12 = 264cm$

We have 12 turns of secondary winding,

The total length of the secondary winding is $l_{sec_winding} = l_{turn} * 12 = 264cm$

The resistance of the winding is

$$R_{pri_winding} = \rho_{Cu} \frac{l_{pri_winding}}{A_{L1}} = 2.3 * 10^{-8} \Omega \cdot m \left(\frac{2.64m}{81.28 * 10^{-6} m^2} \right) = 0.747 m\Omega \quad (366)$$

$$R_{sec_winding} = \rho_{Cu} \frac{l_{sec_winding}}{A_{L2}} = 2.3 * 10^{-8} \Omega \cdot m \left(\frac{2.64m}{40.64 * 10^{-6} m^2} \right) = 1.5 m\Omega \quad (367)$$

$$P_{copper} = I_{L1_rms_peak}^2 \cdot R_{pri_winding} + I_{L2_rms_peak}^2 \cdot R_{sec_winding} = 367^2 * 0.747 * 10^{-3} + 260^2 * 1.5 * 10^{-3} = 202 W \quad (368)$$

5. Total power loss

The total power loss of the Z-source inductor is

$$P_{Lz} = P_{Lz_core} + P_{Lz_winding} = 595 W \quad (369)$$

6. Size and weight

The total size of the inductor is about

$$Vol_{Lz} = 1.35 * 0.55 * 0.9 + 0.7 * 0.8 * 0.15 = 0.75L \quad (370)$$

The total weight of the inductor core is

$$W_{core} = 2.89kg \quad (371)$$

The total weight of the copper is

$$W_{copper} = \rho_{Cu} \cdot (A_{L1} \cdot l_{pri_winding} + A_{L2} \cdot l_{sec_winding}) = 8.9 \text{ g/cm}^3 \cdot (0.4064 \text{ cm}^2 \cdot 264 \text{ cm} + 0.4064 \text{ cm}^2 \cdot 264 \text{ cm}) = 1.9 \text{ kg} \quad (372)$$

$$W_{Lz} = W_{core} + W_{copper} = 4.79 \text{ kg} \quad (373)$$

e. Input Inductor

1. Current Stress

a. Boost mode

During the boost mode, the inverter works as constant power. So the input inductor current is always peak input current which is

$$I_{in_pk} = \frac{P_o}{V_{in}} = \frac{55000}{260} = 211.5 \text{ A} \quad (374)$$

b. Buck mode

In buck mode we work in the constant torque mode which means the output line current will be constant during this mode.

Because we already know

$$I_{in_peak} = \frac{2\sqrt{2}}{\sqrt{3}} \frac{1}{BM} I_{l_rms} \quad (375)$$

Simple boost:

$$I_{in_peak} = \frac{2\sqrt{2}}{\sqrt{3}} \frac{1 - (n+1)D_{op}}{1 - D_{op}} I_{l_rms} \quad (376)$$

Constant boost:

$$I_{in_peak} = \sqrt{2} \frac{1 - (n+1)D_{op}}{1 - D_{op}} I_{l_rms} \quad (377)$$

Maximum boost:

$$I_{in_peak} = \frac{3\sqrt{2}}{\pi} \frac{1 - (n+1)D_{op}}{1 - D_{op}} I_{l_rms} \quad (378)$$

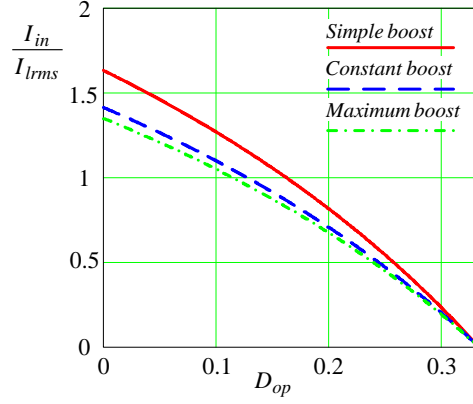


Fig. 70 Input inductor current stress.

So if constant boost control is used, the peak current stress is $1.414 \cdot I_{l_rms} = 212$ A, which is the constant power region current stress.

2. Inductance

Because the inductor switching frequency can be three times higher than the switch switching frequency, so the period of the inductor could be one third of the switch switching period.

a. Boost mode

In boost mode, the output power is the same.

$$L_{in} = \frac{V_{in} D_{sh} T_S}{\Delta I} = \frac{V_{in} \frac{1}{2} T_S}{30\% I_{in}} = \frac{260 * 0.5 * 33.3 \mu}{0.3 * 210} = 69 \mu H$$

b. Buck mode

Input inductance

$$L_{in} = \frac{n V_{in} D_{op} T_S}{\Delta I} = \frac{n V_{in} D_{op} T_S}{30\% I_{in}} \quad (379)$$

Plug in (376), (377), (378) we can get

Simple boost:

$$L_{in} = \frac{n V_{in} D_{op} T_S}{\Delta I} = \frac{\sqrt{3}}{2\sqrt{2}} \frac{n V_{in} D_{op} T_S (1 - D_{op})}{30\% (1 - (n+1) D_{op}) I_{l_rms}} \quad (380)$$

Constant boost

$$L_{in} = \frac{n V_{in} D_{op} T_S}{\Delta I} = \frac{1}{\sqrt{2}} \frac{n V_{in} D_{op} T_S (1 - D_{op})}{30\% (1 - (n+1) D_{op}) I_{l_rms}} \quad (381)$$

Maximum boost:

$$L_{in} = \frac{nV_{in}D_{op}T_S}{\Delta I} = \frac{\pi}{3\sqrt{2}} \frac{nV_{in}D_{op}T_S(1-D_{op})}{30\%(1-(n+1)D_{op})I_{l_rms}} \quad (382)$$

Also make $\frac{V_{in}T_S}{I_{l_rms}2\pi}$ as the base, we can get the normalized input inductance requirement.

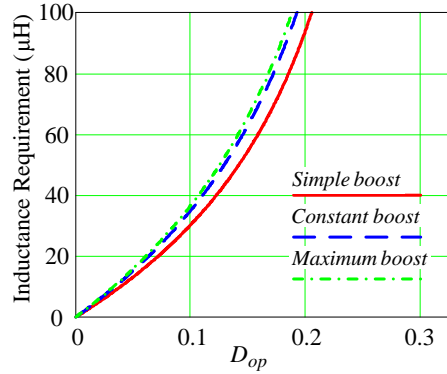


Fig. 71. input inductance requirement of current-fed trans-qZSI with 30% ripple.

Because in the buck mode, the input inductance has to be infinity to meet the current ripple requirement, the inductance value is chosen based on the boost mode, which is 69 uH.

3. Core chosen and core loss

a. Select Core

We decide to choose the core using AP method

$$AP = A_w \cdot A_e = \frac{I_{rms}}{J_{Cu}K_0} \frac{L \cdot I_{peak}}{\Delta B} \quad (383)$$

A_w is the window area

A_e is the cross section area

J_{Cu} is the current density

K_0 is the use of the window coefficient

So

$$AP = A_w \cdot A_e = \frac{I_{rms}}{J_{Cu}K_0} \frac{L \cdot I_{peak}}{\Delta B} = \frac{69\mu * 210^2}{0.3 * 0.0525 * 0.7} = 276 \text{ cm}^4 \quad (384)$$

In order to meet the requirement of AP, we choose the amorphous alloy AMCC320 as our core, The AP of the AMCC320 is as follows,

$$AP_{AMCC320} = 268.3 \text{ cm}^4 \quad (385)$$

b. Number of turns

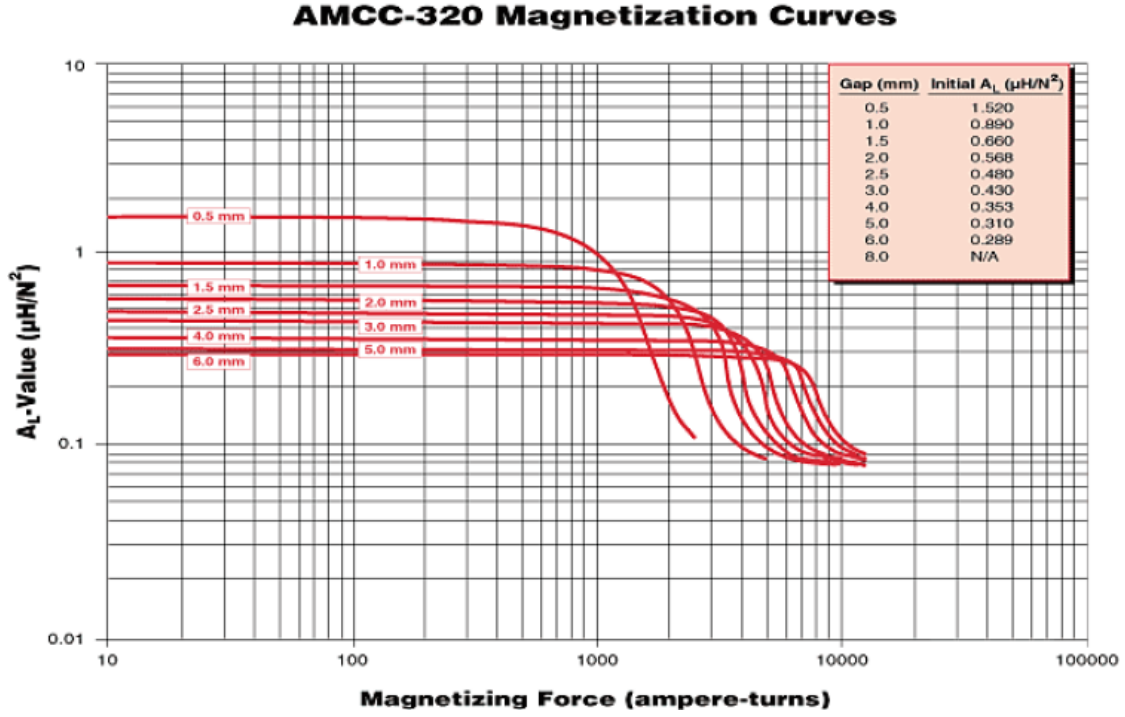


Fig. 72. Inductance value of AMCC-320 core.

We should choose the correct air gap by iteration and 2 mm air gap is finally chosen.

$$A_L \approx 530 \text{ nH} / N^2 \quad (386)$$

So the number of turns is

$$N_T = \sqrt{\frac{L_1}{A_L}} = \sqrt{\frac{69 \mu\text{H}}{0.53 \mu\text{H} / N^2}} = 11.41 \approx 11 \text{ turns} \quad (387)$$

So the Total MMF is

$$\text{MMF} = N_T I_{\text{peak}} = 11 * 210 = 2310 \text{ A-turns} \quad (388)$$

The new A_L after the inductance drop is

$$A_{L_new} \approx 500 \text{ nH} / N^2 \quad (389)$$

So the final inductance value will be

$$L_{1_new} = N_T^2 A_{L_new} = 60.5 \mu\text{H} \quad (390)$$

c. Core size and loss

The total weight of our core is

$$W_{Core} = 2.167 \text{ kg} \quad (391)$$

Because the core loss of AMCC320 is

$$P_L = 6.5B^{1.74}F^{1.51} \quad (392)$$

Fig. 69 shows the core loss curve of this core. B is Tesla, and f is kHz. $P_L = W/kg$. From the figure, we can derive that, when our B=0.3 T $P_{L_30kHz} = 136 \text{ W/kg}$. The total core loss is

$$P_{core_30kHz} = P_{L_30kHz} \cdot W_{core} = 136 \text{ W/kg} * 2.167 \text{ kg} = 294.7 \text{ W} \quad (393)$$

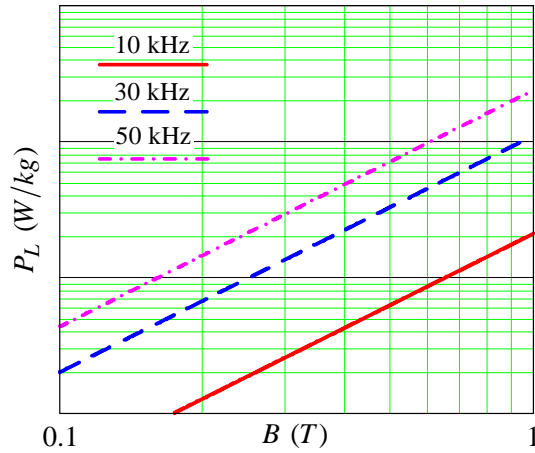


Fig. 73. AMCC320 core loss curve.

4. Winding chosen and copper loss

a. Choose the correct winding size

Because the input inductor current stress is

$$I_{in} = 210 \text{ A} \quad (394)$$

The copper foil is selected for the winding. Assume the current density is

$$J_{Cu} = 5 \text{ A/mm}^2 \quad (395)$$

So the section area of the copper foil should be at least

$$A_{Lin} = \frac{I_{in}}{J_{Cu}} = \frac{210}{5} = 42mm^2 \quad (396)$$

We need to consider the skin effect and calculate the thickness of the copper foil

Because in 100C $\rho_{Cu} = 2.3 \cdot 10^{-8} \Omega \cdot m$, and $\mu_{Cu} = 4\pi \cdot 10^{-7}$, we can calculate the skin depth of the copper in 30 kHz is

$$\delta_{20K} = \sqrt{\frac{\rho_{Cu}}{\pi \mu_{Cu} f_S}} = \sqrt{\frac{2.3 \cdot 10^{-8}}{\pi \cdot 1.257 \cdot 10^{-6} \cdot 30 \cdot 10^3}} = 0.44mm \quad (397)$$

The copper foil with thickness of the 0.016" should be chosen for the design. The width of the copper foil should be chosen according to the window size. The section real area of the copper foil is

$$A_{Lin_1} = 80 \cdot 0.4064 = 32.5 \text{ mm}^2 \quad (398)$$

So the current density is

$$J_{Cu_1} = \frac{I_{in}}{A_{Lin_1}} = 6.5 \text{ A/mm}^2 \quad (399)$$

b. Copper Loss

Because we have 11 turns, for one turn the length of copper could be

$$l_{turn} = 3.7 \cdot 2 + 6.5 \cdot 2 = 20.4cm \quad (400)$$

The total length of the winding is $l_{winding} = l_{turn} \cdot 11 = 224.4cm$

The resistance of the winding is

$$R_{winding} = \rho_{Cu} \frac{l_{winding}}{A_{Lin_1}} = 2.3 \cdot 10^{-8} \Omega \cdot m \frac{2.244m}{32.5 \cdot 10^{-6} m^2} = 1.59m\Omega \quad (401)$$

$$P_{copper} = I_{in}^2 \cdot R_{winding} = 210^2 \cdot 1.59 \cdot 10^{-3} = 70 \text{ W} \quad (402)$$

5. Total power loss

The total power loss of the input inductor is

$$P_{Lin} = P_{Lin_core} + P_{Lin_copper} = 364.8 \text{ W} \quad (403)$$

6. Size and weight

The Total size of the input inductor is about

$$V_{Lin} = 0.79 \cdot 1.29 \cdot 0.5 + 0.8 \cdot 0.1 \cdot 0.7 \cdot 2 + 0.8 \cdot 0.1 \cdot 0.32 \cdot 4 = 0.72L \quad (404)$$

The weight of the input inductor is

$$W_{core} = 2.167kg \quad (405)$$

$$W_{copper} = \rho_{Cu} \cdot A_{Lin_1} \cdot l_{winding} = 8.9g/cm^3 \cdot 0.325cm^2 \cdot 224.4cm = 0.649kg \quad (406)$$

$$W_{Lin} = W_{core} + W_{copper} = 2.167 + 0.649 = 2.816kg \quad (407)$$

f. Output Filter Capacitor

Assume the output capacitor is connected in Δ . And the output voltage ripple is $\pm 10\%$. Because the maximum output peak voltage is 780 V. So our normal output voltage is 700 V peak and about 500 V rms.

1. Voltage Stress

The voltage stress of the output filter capacitor should be the peak output voltage rms value, which should be around 550 V

2. Capacitance [3]

- The output capacitor should be large enough to bypass unwanted CSI line current harmonics.
- The output capacitor should also be small enough to appear as high impedances to the fundamental CSI line currents.

According to the first principle

$$X_{C_{sw}} = \frac{1}{2\pi f_S C_o} \approx 1pu \quad (408)$$

According to the second principle

$$X_C = \frac{1}{2\pi f C_o} \approx 1pu \quad (409)$$

f_S is the switching frequency, and f is the line frequency

The following per phase unit quantities are defined:

$$\text{One per unit voltage} = \frac{500}{\sqrt{3}} = 288 \text{ V} \quad (410)$$

$$\text{one per unit current} = 63.6 \text{ A} \quad (411)$$

$$\text{One per unit impedance } Z = \frac{288}{63.6} \approx 4.5 \quad (412)$$

$$\text{One per unit capacitance } C = \frac{1}{2\pi f \cdot Z} = 589 \mu\text{F} \quad (413)$$

$$\text{One switching per unit capacitance } C_S = \frac{1}{2\pi f_S \cdot Z} = 1.2 \mu\text{F} \quad (414)$$

So the capacitance of the output capacitor is chosen to be 30 uF for one phase, which is in the middle of the capacitance requirement. If the output capacitor is connected in Δ , the required capacitance value will be three times smaller than the Y connection, so the capacitance should be 10 uF.

3. Device chosen

So choose the 5MPA2106J from EC with 530 VAC and 10 uF with 56.6 RMS current stress and 1.5 mOhm ESR.

4. Size and weight

The size of the chosen capacitor is

$$V_C = 3 * \pi * \left(\frac{0.432}{2} \right)^2 * 0.603 = 0.265L \quad (415)$$

The weight of the capacitor is

$$W_{ZC} = 136g * 3 = 408g \quad (416)$$

g. Heatsink

A water cooled heatsink which is about twice bigger than the switch module is chosen.

- Size: $Vol_{\text{heatsink}} = 22 \text{ cm} * 14 \text{ cm} * 1 \text{ cm} = 308 \text{ cm}^3 = 0.308 \text{ L}$
- Weight: 973.5 g

3. Conclusion

Table V provides the summary of device size and weight and power density. Fig. 74 shows the devices size break down. And the Z-source capacitor, Z-source inductor are the major parts of the total converter size.

Table V Summary of device size and weight and power density.

	Switch	Diode	Z-source Capacitor	Z-source Inductor	Input Inductor	Output Capacitor	Heatsink	Total	Power density
Weight(kg)	0.85	0.22	1.2	4.79	2.816	0.408	0.9735	11.2575	4.89kW/kg
Size(L)	0.308	0.09588	0.87	0.75	0.72	0.265	0.308	3.557	15.5kW/L

Fig. 75 shows the total devices weight break down of the 55 kW CF-trans-ZSI, the Z-source inductor is still one of the major parts which contributes most of the weight of the converter. Fig. 76 shows the power loss break down in boost mode, and Fig. 77 shows the power loss break down in buck mode.

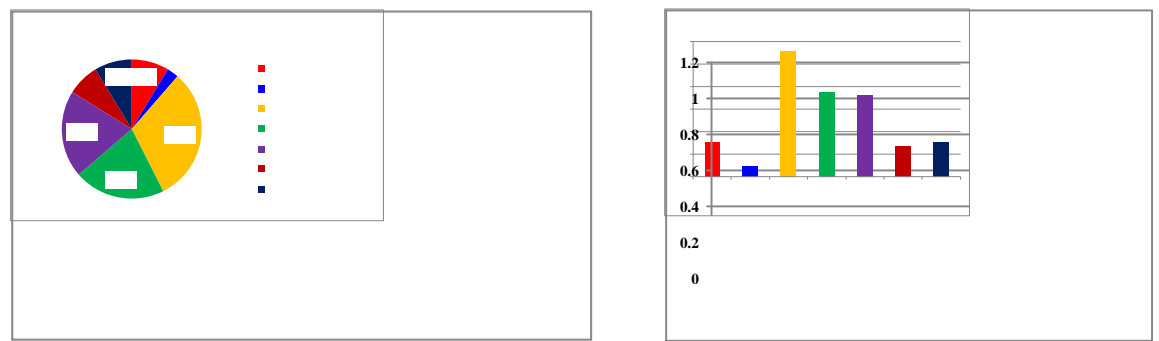


Fig. 74 55 kW CF-trans-qZSI total devices size break down.

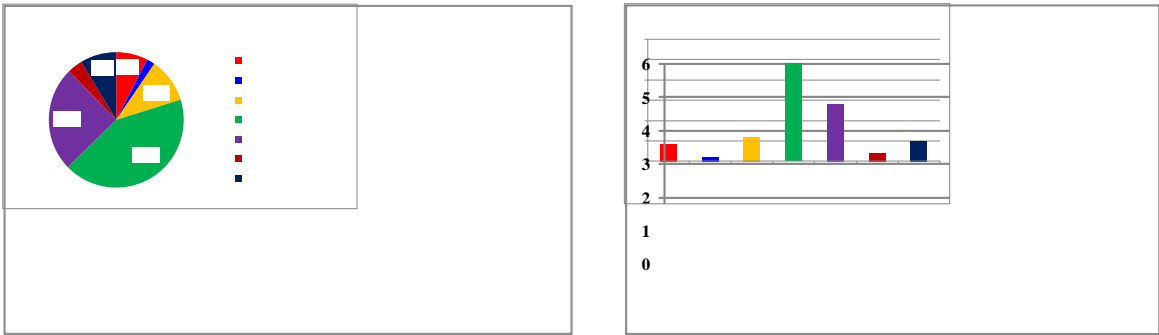


Fig. 75 55 kW CF-trans-qZSI total devices weight break down.

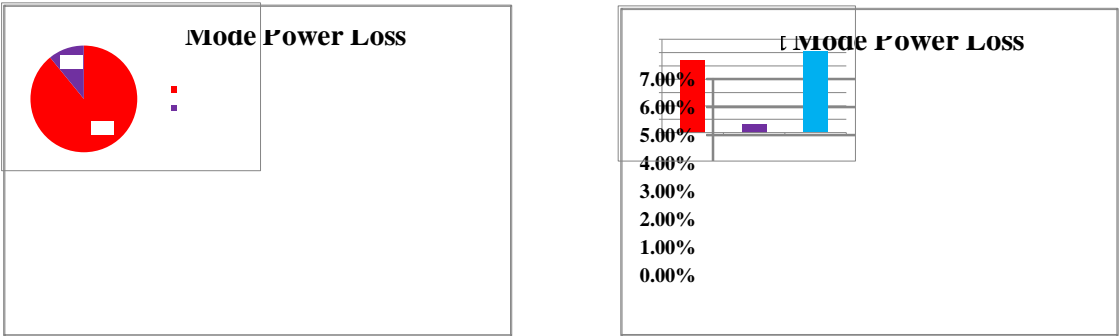


Fig. 76. 55 kW CF-trans-qZSI total devices power loss break down in boost mode.

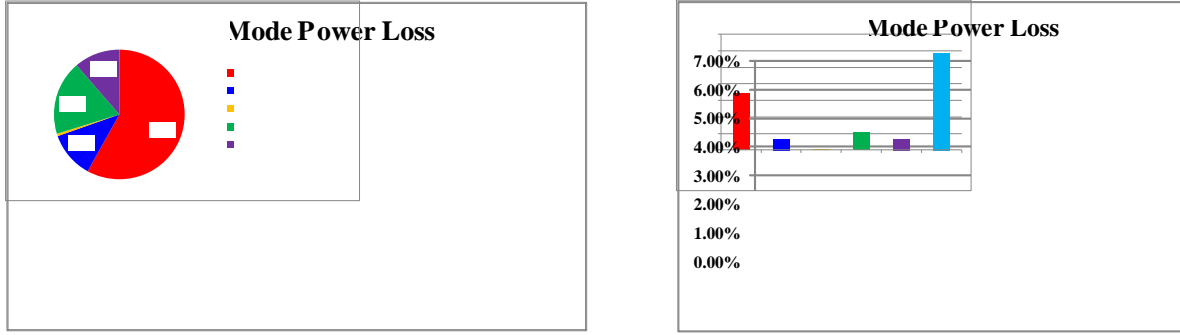


Fig. 77. 55 kW CF-trans-qZSI total devices power loss break down in buck mode.

The switching device power loss is the major part which contributes to the total power loss. In order to achieve higher power density and reduce the size of the inductor, the switching frequency should be increased. But the device switching loss will increase, which will influence the converter efficiency. The RB-IGBT used in this design is still in first generation, with the development of next generation of high frequency switching devices, the total efficiency will increase, the power density will also increase.

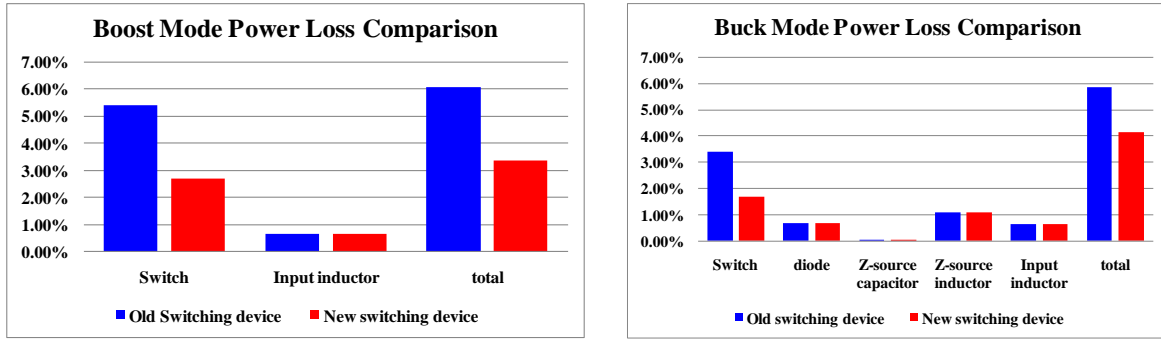


Fig. 78. Power loss comparison of using new switching devices.

- [1] J. R. Espinoza and G. Joos, "Current-source converter on-line pattern generator switching frequency minimization," *Industrial Electronics, IEEE Transactions on*, vol. 44, pp. 198-206, 1997.
- [2] S. Yang, F. Z. Peng, Q. Lei, R. Inoshita, and Z. Qian, "Current-fed Quasi-Z-Source Inverter with Voltage Buck-Boost and Regeneration Capability," in *IEEE Energy Conversion Congress and Exposition, 2009. ECCE 2009.*, San Jose, 2009.
- [3] P. N. Enjeti, P. D. Ziogas, and J. F. Lindsay, "A current source PWM inverter with instantaneous current control capability," *Industry Applications, IEEE Transactions on*, vol. 27, pp. 582-588, 1991.

DISTRIBUTION

Internal

- | | |
|---------------------|-----------------------|
| 1. D. J. Adams | 5. L. D. Marlino |
| 2. K. P. Gambrell | 5. M. Olszewski |
| 3. J. B. Green, Jr. | 6. Laboratory Records |

External

7. R. Al-Attar, DCX, raa9@dcx.com.
8. S. J. Boyd, U.S. Department of Energy, EE-2G/Forrestal Building, 1000 Independence Avenue, S.W., Washington, D.C. 20585.
9. D. Cao, Michigan State University, 2120 Engineering Building, East Lansing, Michigan 48824.
10. J. Czubay, General Motors, john.czubay@gm.com
11. H. Dadkhah, Daimler Chrysler, hd2@ch
12. rysler.com
13. P. B. Davis, U.S. Department of Energy, EE-2G/Forrestal Building, 1000 Independence Avenue, S.W., Washington, D.C. 20585.
14. R. R. Fessler, BIZTEK Consulting, Inc., 820 Roslyn Place, Evanston, Illinois 60201-1724.
15. S. Gopalakrishnan, General Motors Corporation, RMB-356, Mail Code 480-106-390, 30500 Mound Road, Warren, Michigan 48090.
16. G. Hagey, Sentech, Inc., 501 Randolph Street, Williamsburg, Virginia 23185.
17. D. Howell, U.S. Department of Energy, EE-2G/Forrestal Building, 1000 Independence Avenue, S.W., Washington, D.C. 20585.
18. E. Jih, Ford Motor Company, Scientific Research Laboratory, 2101 Village Road, MD-1170, Rm. 2331, Dearborn, Michigan 48121.
19. F. Leonardi, Ford Motor Company, 15050 Commerce Drive, North, Dearborn, Michigan 48120-1261.
20. F. Liang, Ford Motor Company, Scientific Research Laboratory, 2101 Village Road, MD1170, Rm. 2331/SRL, Dearborn, Michigan 48121.
21. M. W. Lloyd, Energetics, Inc., 7164 Columbia Gateway Drive, Columbia, Maryland 21046.
22. F. P. McCluskey, National Renewable Energy Laboratory, 1617 Cole Boulevard, Golden, Colorado 80401.
23. M. Mehall, Ford Motor Company, Scientific Research Laboratory, 2101 Village Road, MD-2247, Rm. 3317, Dearborn, Michigan 48124-2053.
24. N. Olds, United States Council for Automotive Research (USCAR), nolds@uscar.org
25. E. C. Owens, U.S. Department of Energy, EE-2G/Forrestal Building, 1000 Independence Avenue, S.W., Washington, D.C. 20585.
26. F. Z. Peng, Michigan State University, 2120 Engineering Building, East Lansing, Michigan 48824.
27. S. A. Rogers, U.S. Department of Energy, EE-2G/Forrestal Building, 1000 Independence Avenue, S.W., Washington, D.C. 20585.
28. G. S. Smith, General Motors Advanced Technology Center, 3050 Lomita Boulevard, Torrance, California 90505.